Beyond Amyloid and Tau: A Role for Neural Injury and Gliosis in the Pathogenesis of Alzheimer's Disease

By
Andrew P. Merluzzi

A dissertation submitted in partial fulfillment
of the requirements for the degree of

Doctor of Philosophy
(Neuroscience)

at the
UNIVERSITY OF WISCONSIN-MADISON
2018

Date of final oral examination: May 31, 2018

This dissertation is approved by the members of the Final Oral Examination Committee:

Barbara B. Bendlin, Associate Professor, Medicine
Sterling C. Johnson, Professor of Geriatrics and Dementia, Medicine
Luigi Puglielli, Professor, Medicine
Pilar Ossorio, Professor of Law and Bioethics
Andy Alexander, Professor, Medical Physics and Psychiatry

ACKNOWLEDGMENTS

My name sits alone at the top of this document, but everything written here is a reflection of the support I have received in the last several years. I am humbled to see this collaborative effort in its final form.

I appreciate the guidance and insight of my committee, who developed these ideas and saw them through to their place in the scientific canon. I am an improvement on their watch, and I hope I can continue call on them for advice in the future.

During the course of my graduate study, I was privileged to work with the staff and faculty of the Wisconsin ADRC, the Wisconsin Alzheimer's Institute, and collaborators from every corner of the UW – Madison campus. None of this work would have been possible without their hard work and expertise.

I am especially grateful to my unfailingly supportive mentor, Dr. Barbara Bendlin. The Neuroscience and Public Policy program demands many commitments beyond the laboratory, for which I have received nothing but encouragement and wise advice. It is difficult to overstate how privileged I feel to have worked with Barb, both professionally and personally.

Speaking of the personal, I want to thank my friends, near and far. You are my confidants and an endless source of joy. Thank you for appreciating me, for listening to me, for educating me, and most importantly, for tolerating me.

Finally, I would like to thank my brother and parents, to whom this dissertation is dedicated. I know no greater source of generosity and love, and I owe every success to them.

TABLE OF CONTENTS

ABSTRACT

Alzheimer's disease (AD) is characterized by amyloid plaques (Aβ), neurofibrillary tau tangles (NFT), and memory impairments leading to dementia. Yet post-mortem evidence suggests that some individuals with substantial AD neuropathology (Aβ and NFT) did not exhibit dementia during life. This dissertation aims to further elucidate the role of other biological processes in the development of AD – specifically, gliosis, axonal degeneration, and synaptic dysfunction (the latter two of which support structural connectivity). Specifically, this research will address the extent to which gliosis, neural injury, and synaptic dysfunction are requisite for the onset of dementia, the influence of amyloid, neural injury, and gliosis on brain microstructure, and whether biomarkers for these processes can improve our ability to predict subclinical cognitive decline before the onset of dementia. Using cerebrospinal fluid biomarkers attained via lumbar puncture, Aim 1 assesses whether neural injury, synaptic dysfunction, and gliosis contribute to a diagnosis of AD or resilience in the face of significant AD neuropathology. Aim 2 expands on this research, using CSF biomarkers and novel brain imaging techniques to determine the role of AD neuropathology, neural injury, and gliosis on brain microstructure in cognitively healthy, middle-aged adults (hence, earlier in the disease course). Finally, Aim 3 investigates whether these biological processes, when analyzed in conjunction with Aβ and NFT, improve our ability to detect subclinical cognitive decline before the onset of dementia. In sum, this work adds to the growing body of literature implicating processes occurring in conjunction with Aβ and NFT, and provides further insight into the pathophysiology of AD.

CHAPTER 1

Introduction

INTRODUCTION

Alzheimer's disease (AD) is characterized by the accumulation of extracellular amyloid plaques, intracellular neurofibrillary tangles, progressive brain atrophy, and cognitive decline. First described in 1907, Alois Alzheimer presented the case study of Auguste Deter, a 51-year-old patient with early-onset AD (EOAD) characterized by memory loss, delusions, and hallucinations.[1] Post-mortem research has identified the hallmark pathologies of AD: neuritic amyloid plaques (Aβ) and neurofibrillary tau tangles (NFT). [2] While these findings set the foundation for a century of research on AD – including its causes, symptomology, brain pathology, and psychosocial effects – no truly effective treatments are yet available.

The lack of therapeutic progress can be explained by several factors. Historically, clinical trials testing drugs to treat AD have typically taken place in AD patients with frank dementia, who may be too far along in the disease process to respond to treatment.[3] Indeed, multiple lines of research point toward synapse loss as antecedent to cell death and cognitive decline,[4-6] and synaptic dysfunction may be a better predictor of cognitive decline than either amyloid or NFT.[4, 7, 8] Late in the AD process, substantial neuronal dysfunction and death may preclude effective treatment.

As such, it is crucial to examine the AD process early, in what is referred to as the preclinical stage – when an individual has biomarker evidence of incipient AD, but has yet to progress toward cognitive decline and dementia. This stage of the disease represents an opportunity for intervention to delay or prevent mild cognitive impairment (MCI) – the initial symptomatic phase of AD – or dementia itself. Neuropathological

evidence, cerebrospinal fluid biomarkers, as well as molecular imaging, have revealed that amyloid and NFT accumulate years before a decline in memory or executive function.[9]

And yet there may be important processes that occur in addition to the development of amyloid and NFT pathology, and that may contribute to the pathogenesis of AD and cognitive decline.[10] Identifying these biological processes and tracking their progression may prove invaluable for understanding the overall disease course preceding dementia. Specifically, they may provide both targets for intervention and measurable biomarker outcomes for evaluating the success of interventions.[11]

Some such biological phenomena are neural injury, synaptic degeneration, microstructural alterations, and gliosis, which will be described in greater detail later in this document. Post-mortem research has shown that AD brains exhibit significant oxidative stress and gliosis in regions proximate to amyloid plaques and neurofibrillary tangles, possibly contributing to dysfunction at synapses.[12-14] In addition, microstructural abnormalities, which include loss of myelinated axons and synaptic degeneration[15-17], appear to occur independent of cortical pathology in AD. Moreover, biomarker evidence for microstructural abnormalities has been observed at many stages of the disease, including in cognitively healthy adults with biomarker evidence of AD (i.e. Aβ and NFT).[18-21]

This dissertation seeks to further our understanding of neural injury, gliosis, synaptic degeneration in AD. Specifically, this research is centered on determining whether these biological phenomena are phenotypic of or requisite for dementia due to

AD, determine whether and how they relate to white matter microstructure early in the AD progression, and determine whether biomarkers of these biological processes can aid in detecting subclinical cognitive decline before the onset of frank dementia.

The Amyloid Hypothesis

Two characteristic pathologies – amyloid and NFT – underpin much of the Alzheimer's research conducted in the last several decades. The amyloid hypothesis, first outlined by Hardy and Higgins in 1992, describes amyloid as the fundamental causative process in AD[22] and is considered the most parsimonious explanation of AD pathogenesis. As described below, abnormal proteolytic cleavage of the amyloid precursor protein (APP) results in amyloid deposits which form in the intercellular space early in the disease process, sometimes decades before symptoms develop. Advances in Positron Emission Tomography (PET) imaging, including compounds that bind to amyloid plaque (e.g. Pittsburgh Compound B [PiB]), provide *in vivo* evidence that amyloid is present well before the manifestation of cognitive symptoms.[9] PET imaging has played an important role in identifying prodromal AD.[23]

These early deposits are largely non-toxic to neurons. With increasing deposition, plaques increase in size, high concentrations of soluble Aβ in oligomeric form develop, and these oligomers become toxic to nearby pre- and post-synaptic terminals. Referred to as the amyloid cascade, the hypothesis then posits that increasing amyloid deposition and toxicity prompts the local destabilization of tau from microtubules in axons. Through a process not fully elucidated, tau proteins become hyperphosphorylated into paired helical filaments in the axon hillock and dendrites, thereby impairing vesicular transport.

With an increased concentration of vesicles, neuritic swelling and dystrophy occur, increased calcium signaling induces further microtubule destabilization, and the accumulation of vesicles harboring the precursor and proteolytic enzymes that cleave Aβ (amyloid precursor protein [APP], beta-secretase-1 [BACE1] and gamma[γ]-secretase) thereby further accelerate amyloid deposition.[24]

Aβ itself is formed from the cleavage of APP, a widely distributed transmembrane protein. APP is cleaved by several enzymes; in the non-amyloidogenic pathway, α-secretase cleaves APP, producing a membrane-bound fragment and an extracellular fragment, sAPPα. Following this, γ-secretase cleaves the membrane-bound fragment again, producing two non-Aβ protein fragments. Conversely, in the amyloidogenic pathway, APP is first cleaved at a different amino acid location by BACE1. Then, γ-secretase cleavage produces extracellular amyloid fragments ranging in length from 30 to 51 amino acid residues.[25] Aβ38, Aβ40, or Aβ42 are several common isoforms, the latter of which is the most prone to aggregation and is the primary marker of fibrillar amyloid in AD.

Many converging lines of genetic, experimental, and biochemical evidence support the amyloid cascade hypothesis. Among these are: 1) Mutations to the APP protein near or within the Aβ region cause EOAD and are known to increase the production of Aβ42 compared to other amyloid isoforms; 2) a mutation in presenilin 1 or 2 (core proteins of the γ-secretase complex and the catalytic subunits) increases the production of Aβ42 and is the most common cause of EOAD; 3) Down's Syndrome patients have 3 copies of chromosome 21 (and therefore 3 copies of APP), invariably leading to high concentrations

of amyloid plaque, neurofibrillary tangles, dystrophic neurites, and dementia early in life; 4) carriers of the ε4 allele of apolipoprotein E (*APOE*) have decreased clearance of Aβ, leading to increased aggregation and increased risk of dementia due to AD. ε2 carriers, on the other hand, have increased clearance and reduction in the risk of dementia; 5) the oligomeric form of Aβ42 is toxic to neurons, decreasing synaptic density, inhibiting long-term potentiation, and impairing memory in rodents; 6) administration of oligomeric Aβ42 in rodent neurons induces tau hyperphosphorylation and produces dystrophic neurites (Selkoe and Hardy, 2016 provide a review of this evidence[26]).

Alternative Directions

Despite the convergence of evidence in favor of the amyloid hypothesis, other research suggests that Aβ and NFT are necessary but not sufficient for the development of dementia due to AD. For instance, post-mortem studies suggest that a significant number of cognitively normal individuals exhibit substantial Aβ and NFT burden upon autopsy.[27-29] Moreover, molecular neuroimaging studies have shown that PiB binding is observed in upwards of 20-30% of cognitively healthy elderly participants.[30, 31] While these data do not inherently refute the amyloid hypothesis, they complicate the narrative and suggest that Aβ and NFT do not cause dementia in isolation. Therefore, a central goal of this dissertation proposal is to investigate how other biological processes – related to or independent of the characteristic AD neuropathologies – influence diagnosis, brain microstructure, and cognitive trajectories in middle- and older-age individuals.

There are several explanations as to why some individuals can harbor substantial AD neuropathology and yet show no signs of impaired cognition. One often-cited

construct is that lifestyle factors and strategies built over time bestow “cognitive reserve,” thereby allowing individuals to cope with or compensate against increasing AD pathology.[32] A second, related concept is that of “brain reserve,” in which some structural features of the brain confer resilience to dementia, even in the face of substantial Aβ and NFT aggregation[33]). Embedded in each of these hypotheses is the notion that some experiences or physical features of AD-dementia brains differ from non-dementia brains with substantial AD neuropathology. Elucidating these differences may lend insight into the biological processes underlying dementia, the factors underpinning resilience to AD, and novel targets for therapeutic intervention.

One such distinction between the brains of those with AD-dementia versus those who remain cognitively healthy may be the presence of neural injury, synaptic degeneration, and gliosis. Research has demonstrated that neuronal and synaptic degeneration are more strongly correlated with cognitive dysfunction than are the typical AD pathologies [7, 34, 35], and that gliosis can contribute to the pathogenesis of AD[36]. Evidence for these biological phenomena as contributing factors can be found in post-mortem studies. For instance, individuals that harbor significant AD neuropathology, concurrent neural injury abnormalities, and gliosis are more likely to have exhibited dementia during life than those with AD neuropathology alone[27, 37].

CSF biomarker evidence suggests an important role for neural injury in AD. For example, neurofilament light protein (NFL) – a protein expressed principally in large-caliber myelinated axons [38, 39] – is an important component of neuronal cytoarchitecture [40, 41] and is elevated in neurodegenerative diseases, including AD[42-48]. Studies have

shown that increased NFL predicts reduced cognitive performance on the Mini-Mental State Exam (MMSE) in AD patients[49], in line with the fact that these large-caliber myelinated axons are found primarily in temporal and frontal lobes[50]. Further, NFL predicts progression from MCI to frank dementia[49]. These results implicate neural injury as an important biomarker, and perhaps a crucial predictor of cognitive decline before the onset of clinical symptoms.

Other CSF biomarkers of neural injury point to similar conclusions. Neurogranin is a protein expressed in dendrites and dendritic spines[51], and regulates levels of calmodulin following neural excitation and calcium influx[50, 51]. Expressed highest in association cortices and the hippocampus[52], it is involved in plasticity, synaptic regeneration, long-term potentiation, and learning and memory [53]. Synaptic dysfunction is thought to underlie the progression to dementia in AD, and may in fact be a harbinger of neuronal loss [54-56]. Indeed, concentration of synapses in the cortex is reduced by up to 30% even in early stages of AD[4, 57]. Recently, neurogranin has been shown to be reduced in post-mortem brain tissue of AD patients compared to age-matched controls [58], suggesting that it plays a role in cognitive decline. In CSF biomarker studies, neurogranin is elevated in AD and is predictive of cognitive decline and progression to dementia [59, 60]. Reduced levels of neurogranin in post-mortem brains likely reflects the same process of synaptic degeneration as does the increased levels in CSF neurogranin pre-mortem. Research has also shown that individuals with significant Aβ and NFT burden who also have high levels of neurogranin in CSF are likely to have had dementia for only a short duration.

This suggests that elevated neurogranin may be a particularly useful in determining when dementia is temporally proximate [61].

Brain imaging has also provided a window for understanding microstructural alterations in both AD-dementia and preclinical AD. While gray matter changes in AD and preclinical AD are relatively well established – such as reduced hippocampal and cortical volume [62-66] – white matter alterations are emerging as an important factor in the pathogenic process. Altered white matter microstructure is present throughout the AD progression [15, 67-70], and may in fact occur prior to or independently of gray matter changes ([71, 72]; for a review see Sachdev et al., 2013[73]). Magnetic resonance (MR) diffusion-weighted imaging (DWI) is a tool sensitive to the Brownian diffusion of water molecules in the brain, and has been invaluable for making inferences about tissue microstructure in AD *in vivo* [74-79]. Diffusion-tensor imaging (DTI) is the most widely used technique, and provides metrics that include fractional anisotropy (FA) and mean diffusivity (MD), which are sensitive to diffusion parallel to axons and the average diffusion within a voxel, respectively.

It has been shown that CSF biomarkers of AD are associated with decreased FA and increased MD[19], and a voxel-wise analysis in cognitively healthy adults found that AD CSF biomarkers were associated with altered white matter microstructure in several tracts [80]. More recent results using other imaging techniques support the hypothesized link between AD pathology and white matter microstructure. For instance, one study using free-water elimination (FWE) DTI – a novel technique that estimates and removes CSF signal from the diffusion tensor of the tissue – revealed that AD CSF biomarkers were

associated with a higher FWE-DTI *f*-value, indicating greater free water diffusion [81]. In another study, myelin water fraction (MWF) – a quantitative measure sensitive to myelin content – was negatively associated with AD CSF biomarkers, suggesting a more specific link between AD pathology and white matter microstructure [82].

With regard to gliosis, it is known that activated microglia clear cellular debris and Aβ and that astrocytes become activated in the presence of Aβ [83]. Yet the glial cascade may also play a role in neural injury associated with AD. In the presence of an inflammatory trigger such as Aβ, astrocytes and microglia respond by releasing a variety of neurotoxic factors, which further damage surrounding cells [84]. YKL-40 is expressed by activated glia and is elevated with increasing age [85], at all stages of AD [86-88], and is thought to be a marker of Aβ-induced gliosis [86-89]. While amyloid deposition is known to be an early feature of AD, it is thought that the toxic effects on neurons only appear after significant levels of amyloid burden are reached [9]; therefore it may be the case that an active astrocyte or microglial response is necessary for injury to occur. In support of this hypothesis, it has been shown in post-mortem studies that microglial activation, cell death, and degradation of synapses are defining features of AD patients compared to cognitively healthy controls with comparable Aβ and NFT [27].

Despite this evidence, significant gaps in our understanding remain. First, while the roles of gliosis, neural injury, and synaptic dysfunction have been demonstrated post-mortem, it is not fully clear the role that these biological phenomena play during life. Greater insight may lead to an understanding of why Aβ and NFT are necessary but not sufficient for the development of dementia due to AD. If other factors are at work in the

development in dementia, such as gliosis, synaptic dysfunction, and neural injury, can these factors be reliably measured and used diagnostically or prognostically during life?

Second, a more specific understanding of how Aβ, NFT, neural injury, gliosis, and synaptic dysfunction relate to brain microstructure is needed. Despite the usefulness of DTI in AD research, FA and MD may be affected by many physical features, making them non-specific to any particular pathological feature. For example, FA differences can be attributed to alterations in myelination, axonal packing density, axon diameter, or membrane permeability [90]. In light of this, newer DWI acquisition and modeling techniques have sought to improve upon the inferences allowed by DTI and therefore gain a better understanding of brain tissue microstructure in development, aging, and in human disease [91-103]. In this research, novel imaging techniques will be utilized to gain more specific knowledge about how biomarkers of the aforementioned biological processes relate to structural brain changes in AD, such as Neurite Orientation Diffusion and Density Imaging (NODDI).

Finally, while it is known in general that neural injury is involved in AD symptomology, it is not fully clear whether available biomarkers are adequately predictive of cognitive decline. A primary goal of this dissertation is to link neural injury to subclinical cognitive decline before the onset of dementia. This will provide evidence for or against the idea that neural injury biomarkers are useful for assessing disease progression above and beyond what the more typical AD biomarkers (Aβ and NFT) can provide.

Specific Aims

Aim 1: Determine whether neural injury, synaptic dysfunction, and gliosis biomarkers are phenotypic of AD during life. Do these biomarkers add value in distinguishing AD-dementia patients from those with significant Aβ and NFT who remain cognitively unimpaired?

Aim 2: Determine whether AD biomarkers – and AD biomarkers in conjunction with neural injury, synaptic dysfunction, or gliosis – are predictive of white matter microstructure in people at risk for AD.

2A: Determine whether amyloid PET imaging is associated with global and regional white matter microstructure in cognitively unimpaired older adults.

2B: Determine whether CSF biomarkers of neural injury and gliosis are associated with white matter microstructure, particularly in conjunction with Aβ pathology.

Aim 3: Determine which biomarkers of neural injury and synaptic dysfunction add value in predicting cognitive decline within the amyloid, tau, and neurodegeneration [AT(N)] framework.

CHAPTER 2

Neurodegeneration, synaptic dysfunction, and gliosis are phenotypic of Alzheimer's dementia

Neurodegeneration, synaptic dysfunction, and gliosis are phenotypic of Alzheimer's dementia

Andrew P. Merluzzi, BA; Cynthia M. Carlsson, MD; Sterling C. Johnson, PhD; Suzanne E. Schindler, MD, PhD; Sanjay Asthana, MD; Kaj Blennow, MD, PhD; Henrik Zetterberg, MD, PhD; Barbara B. Bendlin, PhD

ABSTRACT:

Objective: To test the hypothesis that cognitively unimpaired individuals with Alzheimer's disease (AD) neuropathology differ from individuals with AD dementia on biomarkers of neurodegeneration, synaptic dysfunction, and glial activation.

Methods: In a cross-sectional study, adult participants above 70 years old (n=79, age=77.1 ± 5.3 years) underwent comprehensive cognitive evaluation and cerebrospinal fluid (CSF) collection, which was assayed for markers of amyloid, phosphorylated tau, neurodegeneration (neurofilament light protein [NFL] and total tau) synaptic dysfunction (neurogranin), and glial activation (YKL-40). Participants were divided into three groups based on diagnosis and p-Tau/$A\beta_{42}$: Those with low p-Tau/$A\beta_{42}$ and unimpaired cognition were classified as "Controls" (n=25); those with high p-Tau/$A\beta_{42}$ diagnosed with AD-dementia or AD-MCI were classified as "AD-Dementia" (n=40); and those with high p-Tau/$A\beta_{42}$ but unimpaired cognition were classified as "Mismatches" (n=14). A similar, secondary analysis was performed with no age exclusion criteria (n=411).

Results: In both the primary and secondary analyses, biomarker levels between groups were compared using ANCOVA while controlling for age and demographic variables. Despite p-Tau/$A\beta_{42}$ and $A\beta_{42}/A\beta_{40}$ levels comparable to the AD-Dementia group, Mismatches had significantly lower levels of NFL and total tau. While not significantly lower than the AD-Dementia group on YKL-40 and neurogranin, Mismatches were also not significantly different from Controls.

Conclusions: These results provide evidence that, in the absence of significant neurodegenerative processes, individuals who harbor AD neuropathology may remain cognitively unimpaired. This provides insight into the biological processes phenotypic of dementia, and supports monitoring multiple biomarkers in individuals positive for AD neuropathology.

ABBREVIATIONS:
AD, Alzheimer's disease; MCI, mild cognitive impairment; NFL, neurofilament light protein; YKL-40, chitinase-3-like protein 1; p-Tau, tau phosphorylated at threonine 181; t-Tau, total tau; WRAP, Wisconsin Registry for Alzheimer's Prevention; APOE4, apolipoprotein E gene ε4

INTRODUCTION

The neuropathology of Alzheimer's disease (AD) – amyloid plaques (Aβ) and neurofibrillary tangles (NFT) – accumulates in a silent phase years before cognitive decline. Remarkably, some individuals live to older age without developing dementia despite substantial AD neuropathology burden upon autopsy, leading some to describe these individuals as "mismatches" [27].

Post-mortem, observed brain differences between AD-Dementia and Mismatch individuals include neuronal dysfunction and glial activation. Neuronal and synaptic degeneration are strongly correlated with cognitive dysfunction[35], and microglial and astrocytic activation is a key feature of the pathogenic process of AD[36].

In the present study, we tested whether cerebrospinal fluid (CSF) biomarkers of neurodegeneration, synaptic dysfunction, and glial activation differ between 1) unimpaired older adults with no biomarker evidence of AD neuropathology (Controls), 2) individuals with AD dementia (AD-Dementia), and 3) cognitively unimpaired individuals with evidence of significant AD neuropathology (Mismatches).

We hypothesized that, compared to cognitively unimpaired older adults with significant AD neuropathology (Mismatches), AD-Dementia participants would exhibit higher NFL, neurogranin, total tau, and YKL-40, indicative of neurodegeneration, synaptic dysfunction, and gliosis.

METHODS

Participants

All participants were recruited from the Wisconsin Registry for Alzheimer's Prevention (WRAP) and the Wisconsin Alzheimer's Disease Research Center (ADRC). These cohorts are composed of unimpaired middle to older-aged adults with and without parents with late onset AD (WRAP), as well as those with AD-MCI and AD-dementia (ADRC). All participants are community dwelling, and underwent examination (including lumbar puncture) at the University of Wisconsin Medical Center between 2010 and 2017. The current sample was enriched for AD risk via a parental history of AD (69%) and included participants positive for the known AD genetic risk factor *Apolipoprotein E* ε4 (*APOE* ε4) (42%). Exclusion criteria included any significant neurological disease other than AD or major psychiatric disorders.

Standard Protocol Approvals, Registrations, and Patient Consents

The University of Wisconsin's institutional review board approved all portions of this study and each participant provided written informed consent before all procedures.

Diagnosis

Participants underwent comprehensive cognitive testing, described previously for WRAP[104] and ADRC[105]. Diagnosis of dementia due to AD or MCI due to AD was determined using National Institute on Aging-Alzheimer's Association (NIA-AA) criteria[106], and reviewed by a multidisciplinary panel of experts at a diagnosis consensus meeting where cognitive testing findings and supporting information gathered at each study visit were reviewed (e.g., self-reported medical history; depressive symptoms; self-reported memory functioning; social history; and informant reports of cognitive and functional

status). Participants included in the final analysis fell into one of three diagnostic categories: 1) cognitively unimpaired, 2) MCI due to AD, or 3) dementia due to AD.

Cerebrospinal Fluid Analyses

CSF collection and assays have been described previously[107]. Cerebrospinal fluid biomarkers were utilized to assess AD-related neuropathology, neuronal dysfunction, and glial activation. We measured $A\beta_{42}$, $A\beta_{40}$, total tau (t-Tau), and tau phosphorylated at threonine 181 (p-Tau), biomarkers that are known to distinguish patients with dementia due to AD from controls[108] and are indicative of conversion from mild cognitive impairment to dementia[109]. In addition to these AD biomarkers, we examined markers of axonal and synaptic neurodegeneration: neurofilament light (NFL) protein and neurogranin, respectively. These biomarkers are associated with cognitive decline and are elevated in AD patients compared to controls[110]. Finally, we measured a marker of activated microglia and astrocytes, chitinase-3-like protein 1 (YKL-40). This protein is elevated in AD, likely as a response to amyloid accumulation and cell injury[87, 88]. We computed and conducted analyses using $A\beta_{42}/A\beta_{40}$, given that it is more closely associated with amyloid plaque burden[111], and p-Tau/$A\beta_{42}$ which is a sensitive marker of AD progression[112].

Statistical Analysis and Group Delineation

Group delineations were made based on cognitive status and CSF biomarker levels, and two analyses were performed. In both analyses, participants were included if they had complete CSF data analyzed and fell into one of three categories: 1) MCI or dementia due to AD ("AD-Dementia"); 2) cognitively unimpaired but with AD neuropathology ("Mismatches"); 3) unimpaired controls without AD neuropathology

("Controls"). The difference between the two analyses is that, in the "age-matched" analysis, groups were limited to 70 years or older, and therefore did not statistically differ on age (tests described below). The second analysis included individuals of any age, where age was controlled for statistically. This is described in the following sections.

Age-Matched Analysis (> 70 Years)

In order to delineate groups of interest, we started with an initial sample comprising 461 participants with a successful lumbar puncture. We then divided the entire sample into quartiles of p-Tau/Aβ_{42}, categorizing the top 25% as phenotypic of AD (n=115) and the remaining 75% of participants as not phenotypic of AD (n=346). Unsurprisingly, the group not phenotypic of AD was substantially younger. In order to account for age as robustly as possible, we limited our primary analysis to individuals aged 70 years or older (n=99 of the original 461) while also including age as a covariate (i.e. the "age-matched" analysis).

Individuals in the top 25% of p-Tau/Aβ_{42} were then divided again based on diagnosis. Participants with a diagnosis of AD-MCI and AD-dementia were categorized as "AD-Dementia". Participants in the top 25% of p-Tau/Aβ_{42} but who were cognitively unimpaired were categorized as "Mismatches." In order to examine a relatively pure AD phenotype, we excluded 20 participants who had an MCI or dementia diagnosis that was deemed unlikely to stem from AD (e.g. frontotemporal dementia), or because they had a p-Tau/Aβ_{42} ratio in the bottom 75% of the entire sample (e.g. not phenotypic of AD, despite a clinical AD diagnosis). This produced a final sample of n=79.

This classification scheme resulted in three groups: 1) low p-Tau/Aβ$_{42}$ and unimpaired cognition classified as “Controls” (n=25); high p-Tau/Aβ$_{42}$ diagnosed with AD-dementia or AD-MCI classified as “AD-Dementia” (n=40); and high p-Tau/Aβ$_{42}$ but unimpaired cognition classified as “Mismatches” (n=14).

Age-Controlled Analysis (Entire Cohort)

A secondary analysis comprised the entire initial sample (n=461, including participants from the age-matched analysis). Control, AD-Dementia, and Mismatch groups were delineated in an identical procedure as outlined above, with the exception that age was not limited to >70. In order to examine a relatively pure AD phenotype, we excluded 50 participants from this 461 who had an MCI or dementia diagnosis that was deemed unlikely to stem from AD (e.g. frontotemporal dementia) or because their p-Tau/Aβ$_{42}$ ratio was in the bottom 75% of the entire sample (e.g. not phenotypic of AD, despite a clinical AD diagnosis). This produced a final sample of n=411.

This classification scheme resulted in three groups: 1) low p-Tau/Aβ$_{42}$ and unimpaired cognition classified as “Controls” (n=291); high p-Tau/Aβ$_{42}$ diagnosed with AD-dementia or AD-MCI classified as “AD-Dementia” (n=61); and high p-Tau/Aβ$_{42}$ but unimpaired cognition classified as “Mismatches” (n=59).

Statistical Analyses

ANCOVA was used to compare the three groups on CSF biomarkers while controlling for demographic variables (years of education, *APOE* ε4 status, family history of AD, sex, and age). Significance was inferred at $\alpha < 0.05$. To achieve normality, NFL, neurogranin, and p-Tau/Aβ$_{42}$ data were log-transformed prior to analysis.

Data Availability:

For purposes of replicating procedures and results, the data used in this study can be made available upon request.

RESULTS

Demographic Characteristics

Age-Matched Analysis (> 70 Years)

Demographic characteristics are displayed in Table 1. An ANOVA comparing demographic variables revealed that groups did not significantly differ on age (as expected). The AD-Dementia group had a significantly lower percentage of female participants compared to Controls ($p=0.046$), and no other groups differed. The AD-Dementia and Mismatch groups had a higher percentage of *APOE* ε4 carriers compared to Controls (p's<0.001). Groups did not differ on family history of AD or education, although we observed a trend for education such that the AD-Dementia group had 1.3 fewer years of education than Controls ($p=0.51$).

Age-Controlled Analysis (Entire Cohort)

Demographic characteristics are displayed in Table 2. The ANOVA comparing demographic variables revealed that groups differed on age at the time of CSF collection (as expected). The AD-Dementia group was 13.3 years older than Controls, and 7.8 years older than the Mismatch group. The Mismatch group was 5.5 years older than Controls (all p's<0.001). The AD-Dementia group had a significantly lower percentage of female participants compared to both the Control and Mismatch groups (p's<0.001). The AD-Dementia ($p<0.001$) and Mismatch ($p=0.003$) groups were more likely to be *APOE* ε4

carriers compared to Controls. The AD-Dementia group was less likely to have a family history of AD at the trend level (p=0.087), likely because many of the younger participants who enroll in the WRAP and ADRC studies do so based on parental family history of AD. Finally, the AD-Dementia group had 0.91 fewer years of education compared to Controls (p=0.034).

Biomarker Comparisons

As expected based on group classification, ANCOVAs for both the age-matched and age-controlled analyses revealed that the AD-Dementia and Mismatch groups had higher levels of p-Tau/$A\beta_{42}$ compared to Controls, but did not differ from each other. Similarly, the AD-Dementia and Mismatch groups had lower levels of $A\beta_{42}/A\beta_{40}$, but did not differ from each other (all p's<0.001, plots not shown).

The group comparison results for NFL varied between the age-matched and age-controlled analyses. Specifically, levels of NFL did not differ significantly between Controls and Mismatches in the age-matched analysis (Figure 1A), with both groups showing reduced levels compared to AD-Dementia (p's <0.001). In the age-controlled analysis (Figure 2A), Mismatches showed intermediate levels of NFL that were significantly higher than Controls but significantly lower than AD-Dementia (p's<0.001).

Neurogranin was consistently elevated in AD-Dementia compared to Controls across both analyses (p's<0.001). In the age-matched analysis (Figure 1B), Mismatches showed qualitatively intermediate values compared to controls and AD-Dementia that did not reach significance. However, in the age-controlled analysis (Figure 2B), Mismatches

showed significantly elevated neurogranin compared to controls ($p<0.001$), and Mismatches were statistically indistinguishable from AD-Dementia.

In the age-matched analysis (Figure 1C), AD-Dementia exhibited higher levels of YKL-40 compared to Controls ($p<0.05$), but there was no statistical difference between Mismatches and either the Control or AD-Dementia groups. In the age-controlled analysis (Figure 2C), the AD-Dementia group exhibited higher levels of YKL-40 compared to both the Control and Mismatch groups (p's <0.001), who did not differ from each other.

In the age-matched analysis (Figure 1D), the AD-Dementia group exhibited higher levels of t-Tau compared to Controls ($p<0.001$) and Mismatches ($p<0.05$), who did not differ from each other. In the age-controlled analysis (Figure 2D), Mismatches showed intermediate levels of t-Tau that were significantly higher than Controls but significantly lower than AD-Dementia (p's <0.001).

DISCUSSION

Some individuals harbor substantial AD neuropathology in the absence of dementia. This raises the question of whether additional biological factors are informative in staging the disease course. Examining cognitively unimpaired individuals with AD-like levels of amyloid and p-Tau (Mismatches), our primary analysis revealed that these individuals had significantly lower NFL and t-Tau compared to AD-Dementia patients. While not significantly lower than AD patients on YKL-40 and neurogranin, Mismatches did not differ significantly from Controls either, suggesting qualitatively intermediate levels of these biomarkers.

NFL, which is expressed principally in large-caliber myelinated axons[38], is an important component of the neuronal cytoskeleton[40, 41]. Studies indicate that increased NFL predicts reduced cognitive performance on the Mini-Mental State Exam in AD patients[49], in line with the fact that these large-caliber myelinated axons are found primarily in temporal and frontal lobes[50] and that NFL is a marker of disease progression[49]. NFL may be a particularly promising biomarker in conjunction with amyloid and tau given that it can be measured in plasma[113]. The results presented in this study underscore the fact that loss of axonal integrity – particularly large-caliber, myelinated axons – plays a role in the development of dementia due to AD.

Neurogranin was elevated in AD-Dementia compared to Controls, and mismatches exhibited qualitatively intermediate values between the AD-Dementia and Control groups in the age-matched analysis. In the larger, age-controlled analysis, the difference between Mismatches and Controls reached statistical significance, with Mismatches showing levels similar to AD-Dementia. Neurogranin is a protein expressed in dendritic spines[51], and regulates levels of calmodulin following action potentials and calcium influx[114]. Expressed highest in associative cortical regions[52], it is implicated in plasticity, synaptic regeneration, long-term potential, and learning and memory[53]. Synaptic dysfunction is thought to underlie the progression to dementia in AD, and may in fact be a harbinger of neuronal loss[54]. Indeed, concentration of synapses in the cortex is reduced by up to 30% even in early stages of AD[5]. Neurogranin is reduced in post-mortem brain tissue of AD patients compared to age-matched controls[115], supporting the idea that it plays a role in cognitive decline. Indeed, the fact that the Mismatch and AD-

Dementia groups had similar levels of neurogranin in both analyses presented here suggests that Mismatches exhibit significant synaptic degeneration despite remaining cognitively unimpaired, and therefore that cognitive impairment may be imminent.

Post-mortem studies also implicate glial activation as a defining feature of dementia due to AD[27, 37]. YKL-40 measured in CSF differs between AD cases and controls[116] and may be a marker of disease progression[86, 117]. The fact that higher levels of YKL-40 were observed in the AD-Dementia group while the Mismatch group had qualitatively intermediate (in the age-matched analysis) or normal levels (in the age-controlled analysis) suggests that gliosis in concert with AD neuropathology may be necessary for the development of dementia due to AD.

Several hypotheses have been put forward to explain why some individuals with significant AD neuropathology remain cognitively unimpaired. Lifestyle factors and cognitive strategies may contribute to cognitive reserve, allowing individuals to function despite AD neuropathology[32]. A related concept is that of brain reserve, where structural or functional features of the brain confer resilience to AD dementia[33]. It is also possible that Mismatches have some genetically conferred immune advantage or environmental influence on immune function that contributes to resilience[118, 119]. Ultimately, it is still unclear why some individuals are more resilient to the damaging effects of AD neuropathology, but elucidating these differences will lend insight into the biological processes underlying resilience and dementia.

Holistically speaking, the AD-Dementia, Control, and Mismatch groups differ on one important characteristic: education. The AD-Dementia group was less educated

compared to Controls at the trend level in the age-matched analysis, and significantly so in the age-controlled analysis. Previous research suggests that education is associated with reduced prevalence of AD-dementia[120, 121]. However, crucially, Mismatches and Controls did not differ on years of education in either analysis presented here. Therefore, Mismatches may be resilient in the face of AD neuropathology when compared to the AD-Dementia group due to cognitive or brain reserve conferred by education or other associated protective factors. One caveat is that the sample overall was highly educated, as well as racially and ethnically homogenous. Therefore, these results may not be applicable to the general population. More research is needed in diverse populations, and improved metrics of education quality – beyond simply years of schooling completed – are needed[122].

We use the term "resilient" with caution when describing the Mismatch group. Cross-sectional data prevent us from concluding that the Mismatch group will remain resilient to dementia as AD neuropathology accumulates. Indeed, the fact that Mismatches exhibited intermediate levels of several biomarkers could suggest a progressively worsening disease state. At the same time, Mismatches may have had an abnormal AD biomarker profile (p-Tau/$A\beta_{42}$) for a shorter length of time than the AD-Dementia group. Still, the results presented here do indicate that – at the time of assessment and at comparable ages to the dementia group – Mismatches appear resilient to cognitive decline despite comparably high levels of AD neuropathology. Longitudinal evaluation is needed for mapping biomarker and cognitive trajectories, as well as for determining the duration of time that Mismatches remain resilient.

Although results are generally consistent between the age-matched analysis and the age-controlled analysis, it is important to note small differences in the patterns of results generated from the two analyses. For example, Mismatches had levels of neurogranin that were qualitatively intermediate between the Control and AD-Dementia groups in the age-matched analysis, but were similar to AD-Dementia and higher than Controls in the age-controlled analysis. This discrepancy is likely attributable to differences in sample size and thus statistical power in the two analyses. While the age-matched analysis further removes any unaccounted-for bias between groups of different ages, the age-controlled analysis increases statistical power to detect differences between groups. Of course, an age-matched analysis with a larger set of participants would be ideal, and longitudinal studies should be the goal of future work.

While longitudinal data will prove invaluable for confirming these findings, this research suggests that larger panels of biomarkers will be useful for differentiating between groups with and without dementia that harbor similar levels of AD neuropathology. Mechanistically, this research adds support to the hypothesis that amyloid and tau are necessary but not sufficient for the onset of frank dementia.

Tables and Figures

Table 1: Table 1: Characteristics of age-matched participants. Values are mean (standard deviation) except where otherwise indicated.

Sample Characteristics	Controls	AD-Dementia	Mismatches	Total
N	25	40	14	79
Age (years)	76.0 (6.5)	78.3 (6.0)	75.8 (4.1)	77.1 (5.3)
Sex (% Female)	64%	35%	71%	51%
APOE ε4 (% Positive)	12%	68%	71%	51%
AD Parental History (% Positive)	40%	45%	71%	48%
Education (Years)	17.0 (2.6)	15.3 (2.9)	16.3 (2.7)	16.0 (2.8)
p-Tau/$A\beta_{42}$	0.05 (0.01)	0.15 (0.07)	0.13 (0.06)	0.12 (0.08)
$A\beta_{42}/A\beta_{40}$	0.11 (0.01)	0.06 (0.01)	0.06 (0.01)	0.08 (0.03)
NFL, pg/mL	879 (279)	1844 (816)	951 (284)	1380 (771)
Neurogranin, pg/mL	312 (140)	567 (352)	384 (134)	454 (291)
YKL-40 ng/mL	192 (67)	264 (73)	207 (63)	233 (75)
Total Tau, pg/mL (t-Tau)	337 (106)	819 (324)	543 (191)	617 (330)

Figure 1: Biomarker plots for age-matched analysis. Each black dot represents one CSF sample from one individual. The bottom of the boxplot represents the 25th percentile, the top represents the 75th percentile (thereby comprising the interquartile range [IQR]), and the middle line represents the median. Whiskers extend 1.5×IQR above the third quartile and 1.5×IQR below the first quartile. The white diamond within the box represents the mean. Panel A: the AD-Dementia group showed significantly higher NFL compared to Controls and Mismatches, who did not differ from each other. Panel B: AD-Dementia exhibited higher levels of neurogranin compared to Controls, and Mismatches did not differ from either Controls or AD-Dementia. Panel C: AD-Dementia exhibited higher levels of YKL-40 compared to Controls, and Mismatches did not differ from either Controls or AD-Dementia. Panel D: the AD-Dementia group exhibited higher levels of t-Tau compared to both Controls and Mismatches, who did not differ from each other. (n.s. denotes no significant difference; ** denotes p<0.001; * denotes p<0.05).

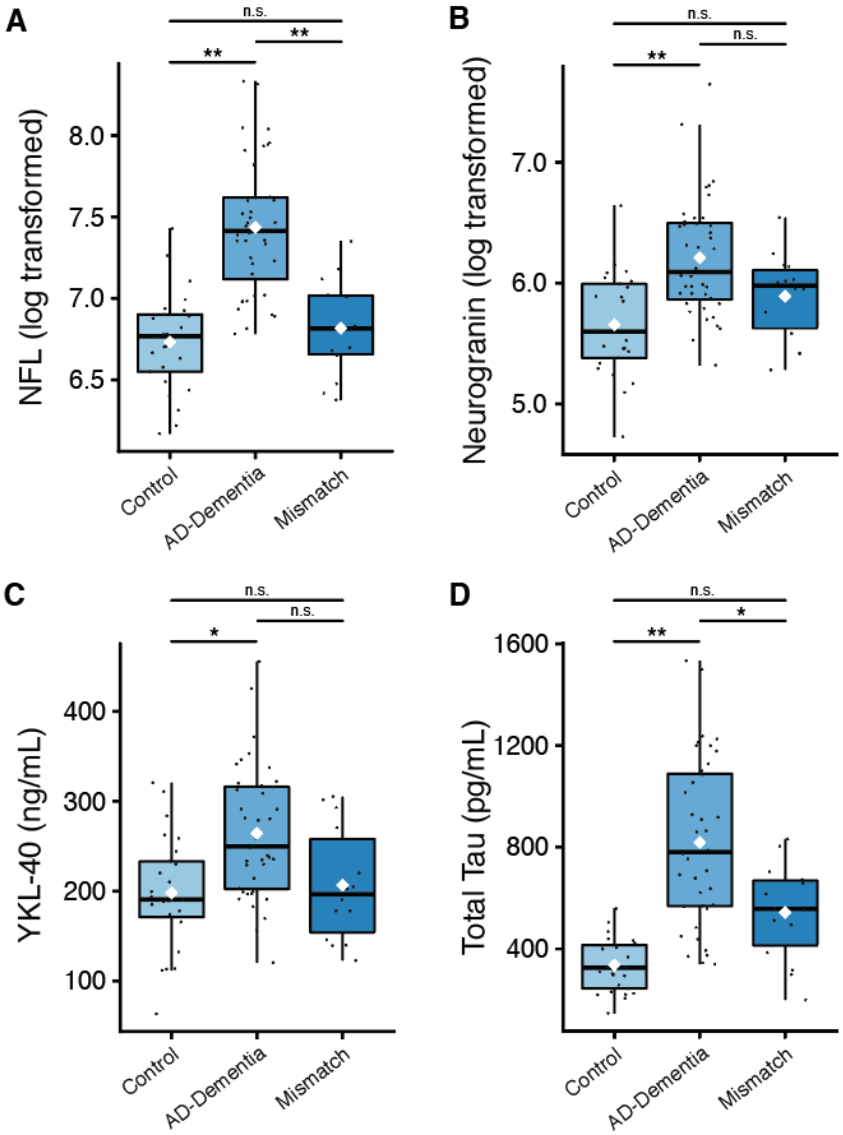

Table 2: Table 2: Characteristics of age-controlled participants. Values are mean (standard deviation) except where otherwise indicated.

Sample Characteristics	Controls	AD-Dementia	Mismatches	Total
N	291	61	59	411
Age (years)	59.9 (7.6)	73.2 (8.9)	65.4 (7.5)	62.7 (9.1)
Sex (% Female)	69%	38%	73%	65%
APOE ε4 (% Positive)	34%	72%	56%	43%
AD Parental History (% Positive)	73%	59%	76%	71%
Education (Years)	16.2 (2.5)	15.3 (2.8)	16.0 (2.6)	16.1 (2.6)
p-Tau/Aβ42	0.05 (0.01)	0.18 (0.08)	0.16 (0.06)	0.09 (0.07)
Aβ42/Aβ40	0.10 (0.02)	0.06 (0.01)	0.06 (0.01)	0.09 (0.02)
NFL, pg/mL	579 (296)	1412 (799)	814 (307)	790 (540)
Neurogranin, pg/mL	309 (159)	576 (323)	441 (144)	367 (214)
YKL-40 ng/mL	151 (51)	196 (77)	159 (53)	159 (65)
Total Tau, pg/mL (t-Tau)	289 (108)	725 (315)	448 (160)	376 (241)

Figure 2: Biomarker plots for age-controlled analysis. Each black dot represents one CSF sample from one individual. The bottom of the boxplot represents the 25th percentile, the top represents the 75th percentile (thereby comprising the interquartile range [IQR]), and the middle line represents the median. Whiskers extend 1.5×IQR above the third quartile and 1.5×IQR below the first quartile. The white diamond within the box represents the mean. Panel A: all groups differed on levels of NFL, with the Mismatch group exhibiting intermediate levels compared to the AD-Dementia and Control groups. Panel B: the AD-Dementia and Mismatch groups did not differ from each other on levels of neurogranin, but both groups had higher levels compared to Controls. Panel C: the AD-Dementia group exhibited higher levels of YKL-40 compared to both Controls and Mismatches, who did not differ from each other. Panel D: all groups differed on levels of t-Tau, with the Mismatch group exhibiting intermediate levels compared to the AD-Dementia and Control groups. (n.s. denotes no significant difference; ** denotes p<0.001; * denotes p<0.05).

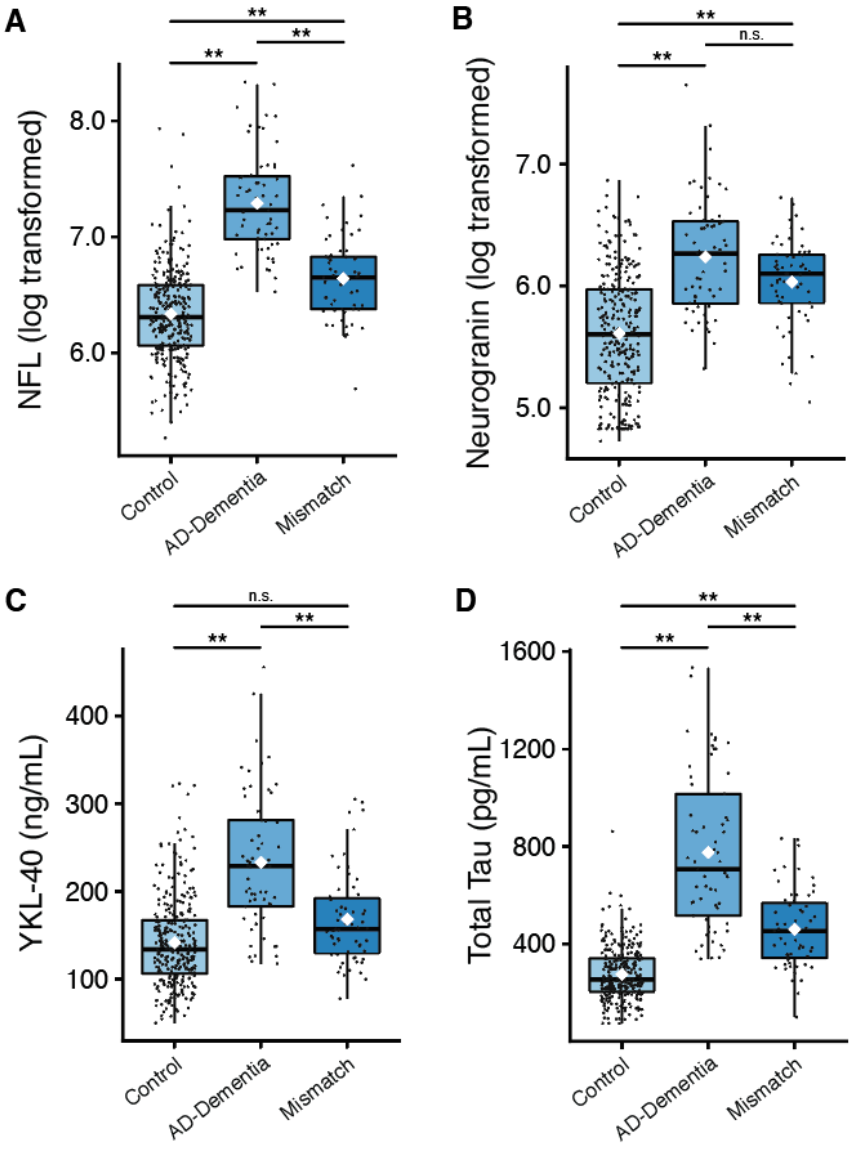

Funding

This project was supported by NIH grants R01AG037639 (BBB), AG027161 (SCJ), P50 AG033514 (SA), the UW Institute for Clinical and Translation Research grant 1UL1RR025011, the Geriatric Research, Education, and Clinical Center (GRECC) of the William S. Middleton Memorial Veterans Hospital, the Swedish Alzheimer Foundation (# AF-553101 and AF-646211), the Torsten Söderberg Foundation (KB), the Research Council of Sweden (project #14002) (KB), the Swedish Brain Foundation (project # FO2015-0021) (KB), LUA/ALF Västra Götalandsregionen (VGR) Sweden (project # ALFGBG-139671) (KB), Swedish Research Council (#2013-2546) (HZ), the European Research Council (#681712) (HZ), Swedish State Support for Clinical Research (#ALFGBG-441051) (HZ), the Knut and Alice Wallenberg Foundation (Wallenberg Academy Fellow 2013) (HZ), and the National Science Foundation Graduate Research Fellowship under Grant No. DGE-1256259 (APM). Any opinions, findings, and conclusions or recommendations expressed in this material are those of the authors(s) and do not necessarily reflect the views of the National Science Foundation.

CHAPTER 3

Amyloid Deposition and Cerebrospinal Fluid Biomarkers are Associated with Altered White Matter Microstructure

Amyloid Deposition and Cerebrospinal Fluid Biomarkers are Associated with Altered White Matter Microstructure

Andrew P. Merluzzi, Douglas C. Dean III, Nagesh Adluru, Nicholas Vogt, Bradley T. Christian, Tobey J. Betthauser, Patrick J. Lao, Sanjay Asthana, Henrik Zetterberg, Kaj Blennow, Sterling C. Johnson, Cynthia M. Carlsson, Mark A. Sager, Andrew L. Alexander, and Barbara B. Bendlin

ABSTRACT

Alzheimer's disease is characterized by progressive accumulation of β-amyloid plaques and neurofibrillary tangles (both of which are cardinal Alzheimer's neuropathologies), as well as neuronal injury and gliosis. While amyloid is assumed to be a neurotoxic instigator of other pathological features of Alzheimer's, the extent to which amyloid accumulation is associated with neural injury in the earliest stages of the disease is unknown. Using multiple linear regression models, we thus investigated whether Alzheimer's-related biomarkers, in particular amyloid – indexed by positron emission tomography (PET) imaging and cerebrospinal fluid (CSF) biomarkers – are associated with neural injury measured with diffusion-weighted imaging. In addition, we examined the possible potentiating effect between biomarkers for axonal degeneration, synaptic dysfunction, and activated glia in conjunction with amyloid. In 67 cognitively unimpaired older participants, we found that higher levels of amyloid deposition measured with [^{11}C]Pittsburgh Compound B (PiB) PET were associated with lower white matter neurite density and orientation dispersion in the hippocampal cingulum and cingulum bundles, though not in a manner that suggests local amyloid toxicity. In addition, in 66 cognitively unimpaired older participants, we observed that higher concentrations of CSF biomarkers – particularly those associated with tau pathology (phosphorylated tau) and activated glia (YKL-40) in conjunction with amyloid – were associated with lower neurite density (NDI) and orientation dispersion (ODI) in similar white matter tracts. These results provide further insight into the mechanisms underlying early brain changes in Alzheimer's, and argue against local toxicity of amyloid early in the Alzheimer's disease process.

ABBREVIATIONS

DTI, Diffusion Tensor Imaging; WRAP, Wisconsin Registry for Alzheimer's Prevention; FA, fractional anisotropy; MD, mean diffusivity; APOE ε4, the varepsilon 4 allele of the apolipoprotein E gene; SPM, Statistical Parametric Mapping; FSL, FMRIB Software Library; BET, Brain Extraction Tool; DTI-TK, Diffusion Tensor Imaging Toolkit; MRI, magnetic resonance imaging; NODDI, neurite orientation dispersion and density imaging; PiB, [^{11}C]Pittsburgh Compound B; NDI, neurite density; ODI, orientation dispersion; F_{iso}, volume fraction of isotropic diffusion; MMSE, Mini-Mental State Examination; LP, lumbar puncture; p-Tau, tau phosphorylated at threonine 181; $A\beta_{42}$, beta-amyloid protein ending in residue 42; $A\beta_{40}$, amyloid-beta protein ending in residue 40; NFL, neurofilament light protein; YKL-40, chitinase-3-like protein 1.

INTRODUCTION

Alzheimer's disease is characterized by accumulation of extracellular amyloid plaques, intracellular neurofibrillary tangles, progressive brain atrophy, and cognitive decline. The extent to which the characteristic pathologies of Alzheimer's are associated with neural injury preceding the onset of dementia remains an ongoing area of research. Gray matter alterations in Alzheimer's and preclinical Alzheimer's are well established, in which Alzheimer's patients exhibit reduced hippocampal and cortical volumes [62-66]. Complementary studies indicate that white matter degradation (loss of myelin or myelinated axons) is present throughout the Alzheimer's progression [15, 67-70], may occur prior to or independently of gray matter changes [71-73], and is possibly manifest before clinical symptom onset [123]. Elucidating these alterations is expected to better inform disease progression, and may also improve staging of Alzheimer's pathology.

Magnetic resonance (MR) diffusion-weighted imaging (DWI) is sensitive to Brownian diffusion of water molecules, and has been invaluable for making inferences about tissue microstructure in Alzheimer's *in vivo* [78, 81, 124, 125]. Diffusion-tensor imaging (DTI) is the most widely used DWI technique, and provides metrics that include fractional anisotropy (FA) and mean diffusivity (MD), which are sensitive to anisotropic and isotropic water diffusion within a voxel. These metrics, however, are non-specific and are affected by many physical features. For example, FA differences can be attributed to alterations in myelination, axonal packing density, axon diameter, or membrane permeability [90]. In light of this, advanced DWI acquisition and modeling techniques have sought to improve upon the inferences allowed by DTI and provide a better understanding of brain tissue

microstructure in development, aging, and in human disease [91-103]. One such DWI modeling technique is Neurite Orientation Diffusion and Density Imaging (NODDI), which models diffusion in a three-compartment fashion, segregating signal from intracellular space (axons and dendrites), extracellular space (diffusion hindered by glial cells and the neuronal soma membranes), and unhindered isotropic diffusion as in cerebrospinal fluid (CSF). To characterize the signal from these diffusion compartments, NODDI relies on MR acquisitions with more diffusion directions and stronger diffusion-weighting gradients (i.e. higher b-values) [126, 127]. This in turn provides quantitative maps indicative of the contributions of these compartments to the overall diffusion within each voxel, providing insight into the underlying tissue microstructure [127-129]. NODDI may provide added value to DTI, revealing specific microstructural changes that are complementary to or independent of changes in DTI metrics [129]. While multi-shell based acquisition and modeling have been used to study brain microstructure in a number of contexts, their application in preclinical Alzheimer's remains limited.

In the present study, we sought to determine the effect of amyloid on neural injury, as indexed by markers sensitive to tissue microstructure. We hypothesized that greater amyloid deposition as indexed by [^{11}C]Pittsburgh Compound B (PiB) binding via positron emission tomography (PET) would be associated with reduced neurite density (NDI), increased orientation dispersion (ODI), and increased volume of isotropic diffusion (F_{iso}) within Alzheimer's-signature white matter tracts (cingulum bundle, hippocampal cingulum, inferior longitudinal fasciculus [ILF], and uncinate fasciculus. We expect, in particular, that alterations in white matter microstructure will be observed in tracts

adjacent to cortical amyloid deposition. Second, we hypothesized that additional biological processes involved in the pathogenesis of Alzheimer's (i.e. those observed to occur in conjunction with amyloid deposition) would lend predictive insight into white matter microstructure alterations. Therefore, we tested the effect of biomarkers for activated glia (chitinase-3-like protein 1 [YKL-40]), synaptic degeneration (neurogranin), and axonal degeneration (neurofilament light protein [NFL]) in combination with $A\beta_{42}$ on white matter microstructure. As a corollary to the NODDI analysis, we also examined FA and MD from the DTI model to determine whether NODDI metrics add value or specificity to these standard diffusion metrics.

In summary, we expected that greater pathological burden (as indexed by higher PiB binding, lower $A\beta_{42}/A\beta_{40}$; higher p-Tau/$A\beta_{42}$, YKL-40/$A\beta_{42}$, neurogranin/$A\beta_{42}$, and NFL/$A\beta_{42}$) would be associated with reduced NDI, increased ODI, increased F_{iso}, decreased FA, and increased MD in white matter tracts important to the clinical symptoms underlying AD.

METHODS

Study Design and Participants

Participants were recruited from the Wisconsin Registry for Alzheimer's Prevention (WRAP) [130] and the Wisconsin Alzheimer's Disease Research Center (ADRC). The cohorts are composed of healthy middle to older-aged adults with and without parents with probable late onset AD. Participants were defined as having a parental history of Alzheimer's if one or both parents were determined to have the disease by medical record review or by a validated informant interview [131], or, rarely, were confirmed as having

dementia due to Alzheimer's by neuropathologic examination. Absence of parental history of Alzheimer's required that the participant's father survive to at least age 70 years and the mother to age 75 years without diagnosis of dementia. Exclusion criteria included any significant neurological disease, MRI contraindications, major psychiatric disorders, or significant mental illness. The University of Wisconsin's Institutional Review Board approved all portions of this study and each participant provided written informed consent before all procedures.

Inclusion in this study was contingent upon several criteria: a successful MRI session in which multiple b-value DWI was acquired; and either a successful lumbar puncture (LP) for CSF or a successful PiB PET scan. With these criteria, 66 people were included in the CSF analyses, and 67 were included in the PiB analyses. Fifty-two of these participants overlapped (i.e. they received both a successful LP and a PiB scan and were included in both analyses). Demographic characteristics and biomarker values are displayed in Table 1 for the PiB analysis, and in Table 2 for the CSF analysis.

Cerebrospinal Fluid Analyses

CSF collection and assays have been described previously [20, 107]. CSF was typically collected on the same day as the MRI, though in some cases CSF was collected at a separate visit (average time between MRI and lumbar puncture = 9.5 days; SD = 28.5 days). In addition to CSF measures of Alzheimer's pathology ($A\beta_{42}$ and p-Tau), assays were performed for NFL, neurogranin, and YKL-40. Higher levels of these markers are indicative of greater axonal degeneration, dendritic degeneration, and astrocyte and/or microglial activation, respectively. In this study we used $A\beta_{42}/A\beta_{40}$ and p-Tau/$A\beta_{42}$

as predictors, given that these ratios are more specific to Alzheimer's pathology [111] and Alzheimer's progression [112, 132, 133]. Moreover, we were particularly interested in the possible potentiating effect of glial activation, synaptic dysfunction, and neural injury coupled with amyloid pathology – phenomena associated with Alzheimer's disease post-mortem [27]. Therefore, ratios of YKL-40/$A\beta_{42}$, neurogranin/$A\beta_{42}$, and NFL/$A\beta_{42}$ were used as predictors.

Pittsburgh Compound-B Positron Emission Tomography

Subjects underwent a 70-minute PiB acquisition on a Siemens ECAT EXACT HR+ PET scanner. Tracer synthesis, PET scanning, and distribution volume map generation have been described previously [20, 134]. PET data were reconstructed using a filtered back-projection algorithm (DIFT) and were corrected for random events, attenuation of annihilation radiation, deadtime, scanner normalization, and scatter radiation and were realigned and coregistered in SPM12 (www.fil.ion.ucl.ac.uk/spm). As described in previous reports from our group, distribution volume ratios (DVRs) were produced with Logan graphical analysis using the cerebellum gray matter as a reference region. Signal was extracted from eight bilateral cortical ROIs (angular gyrus, anterior cingulate gyrus, posterior cingulate cortex, orbitofrontal cortex, precuneus, supramarginal gyrus, middle temporal gyrus, and superior temporal gyrus) then averaged to produce an index of global cortical amyloid burden [135, 136]. To limit the number of contrasts performed, in the present analysis we tested the effect of log-transformed PiB binding in the posterior cingulate cortex (PCC), the orbitofrontal cortex (OFC), and the global PiB measure on alterations in white matter microstructure. In particular, we were interested in whether regional PiB

binding in the OFC and PCC were associated with alterations in white matter microstructure in immediately adjacent tracts, including the cingulum, hippocampal cingulum, ILF, and uncinate fasciculus.

MRI Acquisition

Image acquisition has been described in detail previously [102]. Briefly, participants were imaged on a General Electric 3.0 Tesla MR750 scanner (Waukesha, WI) with an 8-channel head coil. Hybrid Diffusion Imaging (HYDI) [126] was performed using a diffusion-weighted spin-echo echo-planar imaging pulse sequence with 132 DWI measurements spread across 6 q-space shells with the following b-values: 7 repeated volumes at b=0 s/mm^2, 6 directions at b=300 s/mm^2, 21 directions at b=1200 s/mm^2, 24 directions at b=2700 s/mm^2, 24 directions at b=4800 s/mm^2, and 50 directions b=7500 s/mm^2. The remaining parameters include δ = 37.8 ms and Δ = 43.1 ms, TR/TE=6500/102 ms, 96 x 96 matrix over 240 mm FOV with 3 mm thick slices (2.5x2.5x3.0 mm resolution). A separate DWI sequence was performed to acquire DTI metrics. This acquisition scheme is described in the supplementary material.

White matter hyperintensities (WMH) due to presumed ischemia may confound interpretation of DWI results. Therefore, we also collected a three-dimensional T1-weighted inversion recovery prepared fast spoiled gradient-echo image and a T2-weighted fluid attenuated inversion recovery (T2-FLAIR) image, and calculated WMH using the lesion segmentation toolbox2. The ratio of total WMH volume to intracranial volume was used in subsequent analyses. Additional details for these acquisitions and methods are available in the supplementary material.

All images were visually inspected for motion, coverage, and distortion artifacts, but none were excluded on this basis. One participant was excluded due to an enlarged left ventricle that may have negatively influenced image registration.

MRI Processing

Upon acquisition, the DWI data were assessed for motion-related artifacts using DTIPrep (https://www.nitrc.org/projects/dtiprep/), volumes deemed corrupted were removed, image distortions due to eddy currents were corrected using the "eddy" tool [137] as part of the FSL software package (http://fsl.fmrib.ox.ac.uk/fsl/fslwiki/), and diffusion gradients were reoriented using the output transformations from the eddy correction. Brain tissue was then extracted using FSL's Brain Extraction Tool (BET) [138], and tensor fitting was performed using the non-linear estimation tool in CAMINO (http://cmic.cs.ucl.ac.uk/camino/) for spatial normalization purposes. NODDI parameter maps were fit using all the DWI shells in the Matlab toolbox (http://www.nitrc.org/projects/noddi_toolbox) extended to run in parallel on HTCondor (https://github.com/nadluru/NeuroImgMatlabCondor). All NODDI parameter maps were visually inspected in three orthogonal views to assess signal dropout, distortion, or motion, and smoothed at 6mm FWHM. An affine transformation between the population-specific template and the Montreal Neurological Institute (MNI) template was calculated and applied to the NDI, ODI, and F_{iso} images using FSL [139] in order to extract parameter values from regions of interest (ROI). Additional DTI and T1/T2 processing methods are available in the supplementary material.

Region of Interest Definition and Parameter Extraction

ROIs in white matter were defined from the major bundles version of the IIT Human Brain Atlas (v.4.1) [140]. Specifically, bilateral uncinate fasciculus, hippocampal cingulum, cingulum, and ILF were extracted from the full atlas. Several views of these ROIs are depicted in Figure 1. FSLstats (http://www.fsl.fmrib.ox.ac.uk/fsl/fslwiki/Fslutils) was used to extract NDI, ODI, F_{iso}, FA, and MD data from each ROI, and each participants' parameter values for left and right ROIs were averaged (e.g. the mean of the left and right uncinate was used in statistical analyses).

Statistical Analysis

Separate linear regressions with CSF biomarkers ($A\beta_{42}/A\beta_{40}$, p-Tau/$A\beta_{42}$, YKL-40/$A\beta_{42}$, neurogranin/$A\beta_{42}$, and NFL/$A\beta_{42}$) or log-transformed PiB DVRs (global, PCC, and OFC) as predictor variables were performed in SPSS on NDI, ODI, F_{iso}, FA, and MD values from the aforementioned ROIs, controlling for age, sex, *APOE* ε4 genotype, and WMH. Statistical significance was inferred at $p<0.05$, corrected by the number of ROIs (resulting in a threshold of $p<0.0125$).

RESULTS

Biomarker and Microstructure Associations

PiB DVR was associated with altered microstructure, with the full set of contrasts displayed in Table 3 (non-bold cells are significant at $p<0.05$, whereas bold cells remain significant at the corrected threshold). Consistent observations were that PiB DVR in all three ROIs was associated with lower NDI and lower ODI in the cingulum and hippocampal cingulum. Scatterplots of these findings are displayed in Figure 2. No significant results were observed for FA, MD, or F_{iso}.

CSF biomarkers were also associated with altered microstructure, with the full set of contrasts displayed in Table 4 (non-bold cells are significant at $p<0.05$, whereas bold cells remain significant at the corrected threshold). The consistent observations were that p-Tau/$A\beta_{42}$ and YKL-40/$A\beta_{42}$ were associated with lower NDI in all regions, and lower ODI in the cingulum and hippocampal cingulum. Scatterplots for several of these findings are displayed in Figure 3. Other CSF biomarkers were only marginally related to NODDI metrics as shown in Table 4, while no significant results were observed for MD and only one significant result observed for FA (YKL-40/$A\beta_{42}$ was associated with lower FA in the inferior longitudinal fasciculus; $\beta = -0.320$, $p = 0.010$; data not shown).

DISCUSSION

AD is associated with both gross and microscopic brain changes. New advances in *in vivo* imaging are improving our ability to detect these changes in the preclinical stage. In this study, we observed that increased PiB binding and higher levels of p-Tau/$A\beta_{42}$ and YKL-40/$A\beta_{42}$ were associated with lower NDI as well as lower ODI, primarily in the cingulum and hippocampal cingulum. Little to no relationships were observed with FA and MD, suggesting that biophysical models of the acquired DWI signal may prove valuable for a nuanced understanding of microstructural change.

With respect to Alzheimer's pathogenesis, we observed that PiB binding in the PCC and OFC predicted white matter alterations, but interestingly not specifically in white matter tracts adjacent to these cortical regions. This suggests that cortical amyloid accumulation itself does not influence white matter microstructure in connected tracts. That is, a specific biological mechanism for the associations observed here seems

unlikely, given that PiB binding in both ROIs (OFC, PCC) and globally were associated with a reduction in NDI or ODI in the same tracts. Therefore, it seems more likely that amyloid accumulation (indexed by PiB binding) is acting as a "signal" of disease stage, rather than as a direct contributor to alterations in white matter. Other studies bear this out. One recent paper using the Australian Imaging, Biomarkers and Lifestyle (AIBL) dataset found that, in healthy controls and patients with MCI, there was no relationship between amyloid status and fiber density or cross-sectional area for several white matter tracts, including the cingulum. [141]. Our results are in line with this finding and, in sum, suggest a lack of local toxicity of amyloid on adjacent white matter tracts.

With respect to neuronal functioning, it is interesting to note that studies using fluorodeoxyglucose [^{18}F]FDG PET imaging have shown that local amyloid accumulation appears to be relatively independent of reductions in glucose metabolism in overlapping regions [142]. One hypothesis is that white matter alterations of the sort observed here later influence neuronal function and glucose metabolism, although carefully constructed longitudinal studies would be required to address this question.

It is also possible that the relationship between amyloid deposition and white matter microstructure is mediated by neurofibrillary tangle accumulation, or that it predicts later tangle accumulation. Indeed, a recent study suggests that increased amyloid deposition strengthens the association between microstructural pathology in the hippocampal cingulum and tau in the posterior cingulate cortex [143]. Future studies should investigate this further.

The CSF results presented here suggest that YKL-40/$A\beta_{42}$ and p-Tau/$A\beta_{42}$ appear to be the strongest predictors of alterations in white matter microstructure. Activated microglia and astrocytes clear cellular debris and Aβ, although this biochemical cascade may also play a role in neural damage associated with AD. In the presence of a trigger such as Aβ, glia may respond by releasing neurotoxic factors, which further damage surrounding cells [84]. YKL-40 is expressed by activated microglia and astrocytes and is elevated with increasing age [85] and at all stages of Alzheimer's [86-88]. Given that few associations were observed for $A\beta_{42}/A\beta_{40}$ (and none surviving correction), these results suggest that the coupling of glial activation and amyloid plays an important role in microstructural alterations in this population. While amyloid deposition is known to be an early feature of AD, it is thought that the toxic effects on neurons only appear after significant levels of amyloid burden are reached [9], which is one hypothesis as to why we observed significant associations between microstructure and PiB but not $A\beta_{42}/A\beta_{40}$. It may be the case that early increases in amyloid do not associate with microstructure unless an active glial response is also present. In support of this hypothesis, post-mortem studies indicate that glial activation, cell death, and degradation of synapses are defining features of Alzheimer's dementia [27].

With respect to p-Tau/$A\beta_{42}$, the present results provide some replication and validation of previous studies examining CSF biomarkers and DWI in cognitively healthy older adults. CSF $A\beta_{42}$, p-Tau, or their ratio are associated with decreased FA and increased MD [19, 80]. While we did not observe significant associations for FA or MD here, the NODDI findings may explain this (described in detail below). Recent results from our

group using other imaging techniques also support the hypothesized link between Alzheimer's pathology and white matter microstructure. Myelin water fraction – a quantitative measure sensitive to myelin content – was negatively associated with p-Tau/$A\beta_{42}$, suggesting a more specific link between Alzheimer's pathology and white matter microstructure [82].

The lack of robust findings for neurogranin/$A\beta_{42}$ and NFL/$A\beta_{42}$ was unexpected. Several explanations may account for this. First, these biomarkers may not associate with subtle brain changes in early stages of AD. Because this cohort was relatively young and cognitively healthy, large microstructural alterations are not expected. Perhaps later in the disease process, when brain injury is more pronounced, the relationship between markers of neural injury and cross-sectional DWI would be stronger. Indeed, neurogranin has been shown to predict longitudinal changes in FA and MD [144], and both neurogranin and NFL are elevated in Alzheimer's patients and prodromal Alzheimer's [110, 145-147].

In both the PiB and CSF analyses, lower ODI was unexpected given that higher ODI has been observed in aging [97]. Perhaps the most parsimonious explanation of this finding is that it represents a loss of diverging fibers from branching connections or crossing fibers, which are ubiquitous throughout cerebral white matter [148]. A loss of diverging fibers would be consistent with a reduction in both NDI and ODI, and a recent study examining early-onset Alzheimer's supports such a hypothesis [149]. In addition, it is likely that a reduction in NDI and ODI simultaneously impacts FA in diverging directions, perhaps accounting for the fact that we did not observe associations in FA in the present study. This further supports the notion that biophysical models may be more indicative of

underlying microstructure than tensor models. The lack of F_{iso} or MD findings was also unexpected, although minimal associations with these metrics have been observed in other contexts [129, 149]. It is possible that these diffusion metrics may be more sensitive to gross neurodegeneration rather than subtle alterations in microstructure associated with biomarkers in cognitively unimpaired participants at risk for AD.

Several limitations of this study deserve note. First, the NODDI model assumes that microstructural diffusion can be segregated into three components, while also making the assumption that diffusion is entirely restricted within the neurite compartment. Further work into the validity of these assumptions is needed, particularly in the context of the idiosyncratic brain injury processes characteristic of various diseases, and also with human histopathological evidence. However, NODDI measures have been validated against immunohistological measures of neurite microstructure in a mouse model [150] and applied with relatively consistent results in aging and clinical populations [128, 129, 151, 152].

The sample under study here was relatively homogenous with respect to demographics (largely Caucasian, female, and highly educated). Future studies with larger populations may have more power to detect subtle associations between biomarkers and white matter microstructure using biophysical DWI models. In addition, it remains to be seen whether the white matter alterations observed in the present study are predictive of cognitive decline in this healthy population, but longitudinal studies may bear this hypothesis out.

In summary, these findings support the notion that regional PiB does not correlate robustly with local alterations in white matter microstructure, but rather acts as a proxy of

other accompanying changes in the Alzheimer's process, including white matter alterations. In addition, the CSF findings presented here provide evidence that pathology accompanying accumulating amyloid (i.e. activated glia or neurofibrillary tangles) is requisite for observing white matter microstructural change in a way that evidence of amyloidosis in CSF ($A\beta_{42}/A\beta_{40}$) does not. These data underscore the importance of investigating white matter changes in the preclinical stage. Determining the course of microstructural alterations in Alzheimer's with sensitive MR, PET, and CSF based measures may lend further insight into the staging of the disease and provide a foundation for future interventions.

Acknowledgements

The authors acknowledge the support of researchers and staff at the Waisman Center and the Wisconsin Institute for Medical Research at the University of Wisconsin-Madison, where imaging data were collected. Finally, the authors thank their dedicated participants for their valuable time.

Funding

This project was supported by NIH grants R01AG037639 (BBB), AG027161 (SCJ), P50 AG033514 (SA), K99MH110596 (DCD), R01 AG054059 (PI, Carey Gleason, PhD) and U54 HD090256 (Waisman Center), the UW Institute for Clinical and Translation Research grant 1UL1RR025011, the Geriatric Research, Education, and Clinical Center (GRECC) of the William S. Middleton Memorial Veterans Hospital, the Swedish Alzheimer Foundation (# AF-553101 and AF-646211), the Torsten Söderberg Foundation (KB), the Research Council of Sweden (project #14002) (KB), the Swedish Brain Foundation

(project # FO2015-0021) (KB), LUA/ALF Västra Götalandsregionen (VGR) Sweden (project # ALFGBG-139671) (KB), Swedish Research Council (#2013-2546) (HZ), the European Research Council (#681712) (HZ), Swedish State Support for Clinical Research (#ALFGBG-441051) (HZ), the Knut and Alice Wallenberg Foundation (Wallenberg Academy Fellow 2013) (HZ), and the National Science Foundation Graduate Research Fellowship under Grant No. DGE-1256259 (APM). Any opinions, findings, and conclusions or recommendations expressed in this material are those of the authors(s) and do not necessarily reflect the views of the National Science Foundation.

SUPPLEMENTAL METHODS

Diffusion Tensor Imaging Methods

Acquisition: Participants were imaged on a General Electric 3.0 T Discovery MR750 (Waukesha, WI) MRI system with an 8-channel head coil and parallel imaging with ASSET (R = 2). DTI was acquired using a diffusion-weighted, spin-echo, single-shot, echo planar imaging pulse sequence in 40 encoding directions, b-value = 1300 s/mm2, with eight non-diffusion-weighted (b = 0) reference images. The cerebrum was covered using contiguous 2.5 mm thick axial slices, FOV = 24 cm, TR = 8000 ms, TE = 67.8, matrix = 96 × 96, resulting in isotropic 2.5 mm3 voxels. High order shimming was performed prior to the DTI acquisition to optimize the homogeneity of the magnetic field across the brain and to minimize EPI distortions[153].

Processing: First, head motion and image distortions (stretches and shears) due to eddy currents were corrected with affine transformation in the FSL (FMRIB Software Library) package (http://www.fmrib.ox.ac.uk/fsl/) and diffusion gradients were reoriented

using the output transformations from the eddy correction in FSL. Geometric distortion from the inhomogeneous magnetic field applied was corrected with a B0 field map and PRELUDE (phase region expanding labeler for unwrapping discrete estimates) and FUGUE (FMRIB's utility for geometrically unwarping EPIs) from FSL. Brain tissue was extracted using FSL's BET (Brain Extraction Tool). Tensor fitting was performed using a nonlinear least squares method in CAMINO (http://cmic.cs.ucl.ac.uk/camino/). Individual maps were registered to a population specific template constructed using Diffusion Tensor Imaging Toolkit (DTI-TK) (http://www.nitrc.org/projects/dtitk/) which is an optimized DTI spatial normalization and atlas construction tool[154, 155] that has been shown to perform superior registration compared to scalar based registration methods[156]. Spatial normalization was performed using a diffeomorphic registration method[17] that incrementally estimates the displacement field using a tensor-based registration formulation. All DTI parameter maps were visually inspected in three orthogonal views to assess signal dropout, distortion, or motion, and smoothed at 6mm FWHM. An affine transformation between the population-specific template and the Montreal Neurological Institute (MNI) template was calculated and applied to the FA and MD images using FSL [139] in order to extract parameter values from regions of interest (ROI).

T1/T2 Imaging and White Matter Hyperintensity Methods

Acquisition: The imaging protocol consisted of a 3D T1-weighted inversion recovery prepared fast spoiled gradient-echo image and a T2-weighted fluid attenuated inversion recovery (T2-FLAIR) image. 3D T1-weighted images were acquired in the axial plane with the following parameters: inversion time (TI) = 450 ms; repetition time (TR) =

8.1 ms; echo time (TE) = 3.2 ms; NEX = 1; flip angle = 12°; acquisition matrix = 256 x 256 x 156; FOV = 256 mm; slice thickness = 1.0 mm no gap. 3D T2-weighted fluid attenuated inversion recovery (FLAIR) images were acquired in the sagittal plane using the following parameters: TI = 1869 ms; TR = 6000 ms; TE = 123 ms; flip angle = 90°; acquisition matrix = 256 x 256 x 100, FOV = 256 mm; slice thickness = 2.0 mm no gap.

Processing: White matter hyperintensity (WMH) segmentation was achieved using the T1-weighted and T2-weighted images and the Lesion Segmentation Toolbox (LST) version 1.2.2 in SPM8 (http://www.fil.ion.ucl.ac.uk/spm/) [157]. Specifically, lesions were seeded based on spatial and intensity probabilities from T1-weighted images and hyperintense outliers on T2-FLAIR images, a method that has been validated with high agreement (R^2 = 0.94) to manual tracing [157]. When controlling for possible effects of WMH, global WMH was included in all statistical models as a ratio to intracranial volume (ICV). ICV was calculated using a "reverse brain masking" method [158]. Using segmentation procedures in SPM12, gray matter, white matter, and CSF International Consortium for Brain Mapping (ICBM) probability maps were created and then summed to produce an ICV probability map. Then, the inverse deformation field resulting from unified segmentation on each image was applied to the ICV probability map, in order to produce an ICV mask. A threshold of 90% was applied to this participant-specific ICV probability map and the total volume was extracted. To control for variability in head size, the WMH variable was divided by ICV and multiplied by 100 to give a ratio (WMHr) in units of percent of ICV.

Tables and Figures

Figure 1: Several images depicting white matter regions of interest (ROIs) used in the present study. Green = uncinate fasciculus. Blue = cingulum. Red = hippocampal cingulum. Yellow = inferior longitudinal fasciculus.

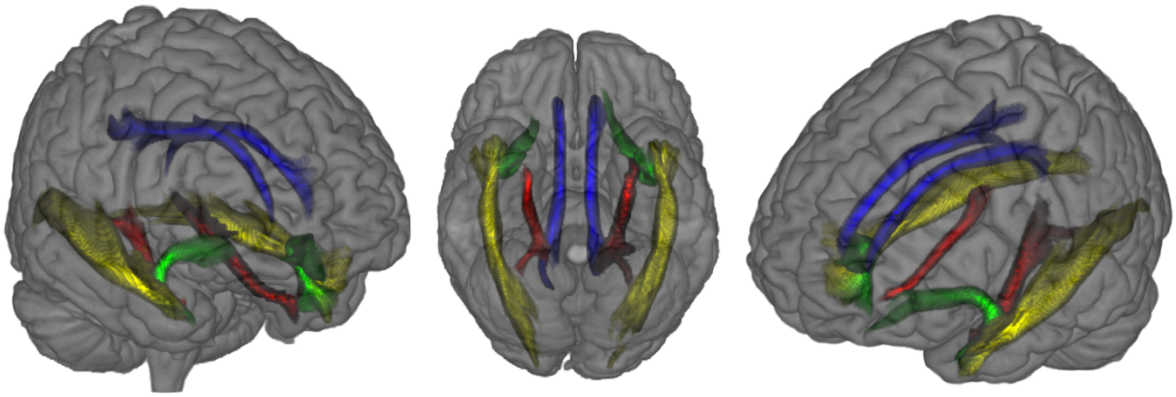

Table 1: Demographic characteristics of participants included in the PiB analysis. All values are MEAN (SD) unless otherwise indicated.

Sample Characteristics	Total
N	67
Age at MRI (years)	62.2 (5.9)
Sex (% Female)	63%
APOE ε4 (% Positive)	40%
Alzheimer's Parental History (% Positive)	69%
Mini Mental State Examination (MMSE)	29.2 (1.1)
Education (Years)	17.0 (2.5)
PCC PiB (DVR)	1.32 (0.22)
OFC PiB (DVR)	1.13 (0.22)
Total PiB (DVR)	1.15 (0.16)

Table 1 Abbreviations: APOE ε4, the varepsilon 4 allele of the apolipoprotein E gene; MRI, magnetic resonance imaging; MMSE, Mini-Mental State Examination; PCC, posterior cingulate cortex; OFC, orbitofrontal cortex; PiB, [^{11}C]Pittsburgh Compound B; DVR, distribution volume ratio

Table 2: Demographic characteristics of participants included in the CSF analysis. All values are MEAN (SD) unless otherwise indicated.

Sample Characteristics	Total
N	66
Age at MRI (years)	61.9 (6.2)
Sex (% Female)	71%
APOE ε4 (% Positive)	41%
Alzheimer's Parental History (% Positive)	74%
Mini Mental State Examination (MMSE)	29.3 (1.1)
Education (Years)	16.8 (2.3)
p-Tau/$A\beta_{42}$	0.06 (0.03)
$A\beta_{42}/A\beta_{40}$	0.10 (0.02)
NFL/$A\beta_{42}$	0.88 (0.42)
Neurogranin/$A\beta_{42}$	0.55 (0.36)
YKL-40/$A\beta_{42}$	0.23 (0.10)

Table 2 Abbreviations: APOE ε4, the varepsilon 4 allele of the apolipoprotein E gene; MRI, magnetic resonance imaging; MMSE, Mini-Mental State Examination; p-Tau, tau phosphorylated at threonine 181; $A\beta_{42}$, beta-amyloid protein ending in residue 42; $A\beta_{40}$, amyloid-beta protein ending in residue 40; NFL, neurofilament light protein; YKL-40, chitinase-3-like protein 1.

Table 3: Results table for regressions between amyloid deposition indexed by PiB and NODDI metrics (NDI, ODI, F_{iso}), with beta-values and p-values displayed for significant associations. Non-bold cells are significant at $p<0.05$, and bold cells remain significant at the corrected threshold ($p<0.0125$). Dashes indicate non-significant relationships.

Amyloid Biomarker	NDI Cingulum	NDI HC Cingulum	NDI Uncinate	NDI ILF	ODI Cingulum	ODI HC Cingulum	ODI Uncinate	ODI ILF	Fiso Cingulum	Fiso HC Cingulum	Fiso Uncinate	Fiso ILF
Global PiB	β = -.294 p = 0.018	**β = -.397 p = 0.001**	–	–	**β = -.456 p < 0.001**	**β = -.421 p < 0.001**	–	–	–	–	–	–
PCC PiB	**β = -.345 p = 0.005**	**β = -.406 p = 0.001**	**β = -.351 p = 0.004**	–	β = -.310 p = 0.013	**β = -.313 p = 0.012**	–	–	–	–	–	–
OFC PiB	**β = -.335 p = 0.007**	**β = -.399 p = 0.001**	–	–	**β = -.463 p < 0.001**	**β = -.410 p = 0.001**	–	–	–	–	–	–

Table 3 Abbreviations: PCC, posterior cingulate cortex; OFC, orbitofrontal cortex; PiB, [^{11}C]Pittsburgh Compound B; NDI, neurite density; ODI, orientation dispersion; F_{iso}, volume fraction of isotropic diffusion; HC Cingulum, hippocampal cingulum; ILF, inferior longitudinal fasciculus

Table 4: Results table for regressions between CSF biomarkers and NODDI metrics (NDI, ODI, F_{iso}), with beta-values and p-values displayed for significant associations. Non-bold cells are significant at $p<0.05$, and bold cells remain significant at the corrected threshold ($p<0.0125$). Dashes indicate non-significant relationships.

CSF Biomarker	NDI Cingulum	NDI HC Cingulum	NDI Uncinate	NDI ILF	ODI Cingulum	ODI HC Cingulum	ODI Uncinate	ODI ILF	Fiso Cingulum	Fiso HC Cingulum	Fiso Uncinate	Fiso ILF
Aβ42/Aβ40	β = .270 p = 0.032	–	–	–	–	–	–	–	β = -.264 p = 0.036	–	β = -.272 p = 0.031	–
p-Tau/Aβ42	**β = -.345 p = 0.006**	**β = -.358 p = 0.004**	β = -.309 p = 0.014	β = -.302 p = 0.016	β = -.291 p = 0.021	**β = -.315 p = 0.012**	–	–	–	–	–	–
YKL-40/Aβ42	β = -.294 p = 0.019	**β = -.359 p = 0.004**	**β = -.328 p = 0.009**	**β = -.341 p = 0.006**	**β = -.360 p = 0.004**	**β = -.385 p = 0.002**	–	–	–	–	–	–
NG/Aβ42	–	–	–	–	β = -.266 p = 0.035	–	–	–	–	–	–	–
NFL/Aβ42	–	–	–	–	–	**β = -.366 p = 0.003**	–	–	–	–	–	–

Table 4 Abbreviations: NDI, neurite density; ODI, orientation dispersion; F_{iso}, volume fraction of isotropic diffusion; HC Cingulum, hippocampal cingulum; ILF, inferior longitudinal fasciculus; p-Tau, tau phosphorylated at threonine 181; $A\beta_{42}$, beta-amyloid protein ending in residue 42; $A\beta_{40}$, amyloid-beta protein ending in residue 40; NFL, neurofilament light protein; YKL-40, chitinase-3-like protein 1.

Figure 2: Scatterplots of significant associations between amyloid deposition and neurite density (NDI, light blue) or orientation dispersion (ODI, dark blue) in hippocampal cingulum and cingulum ROIs.

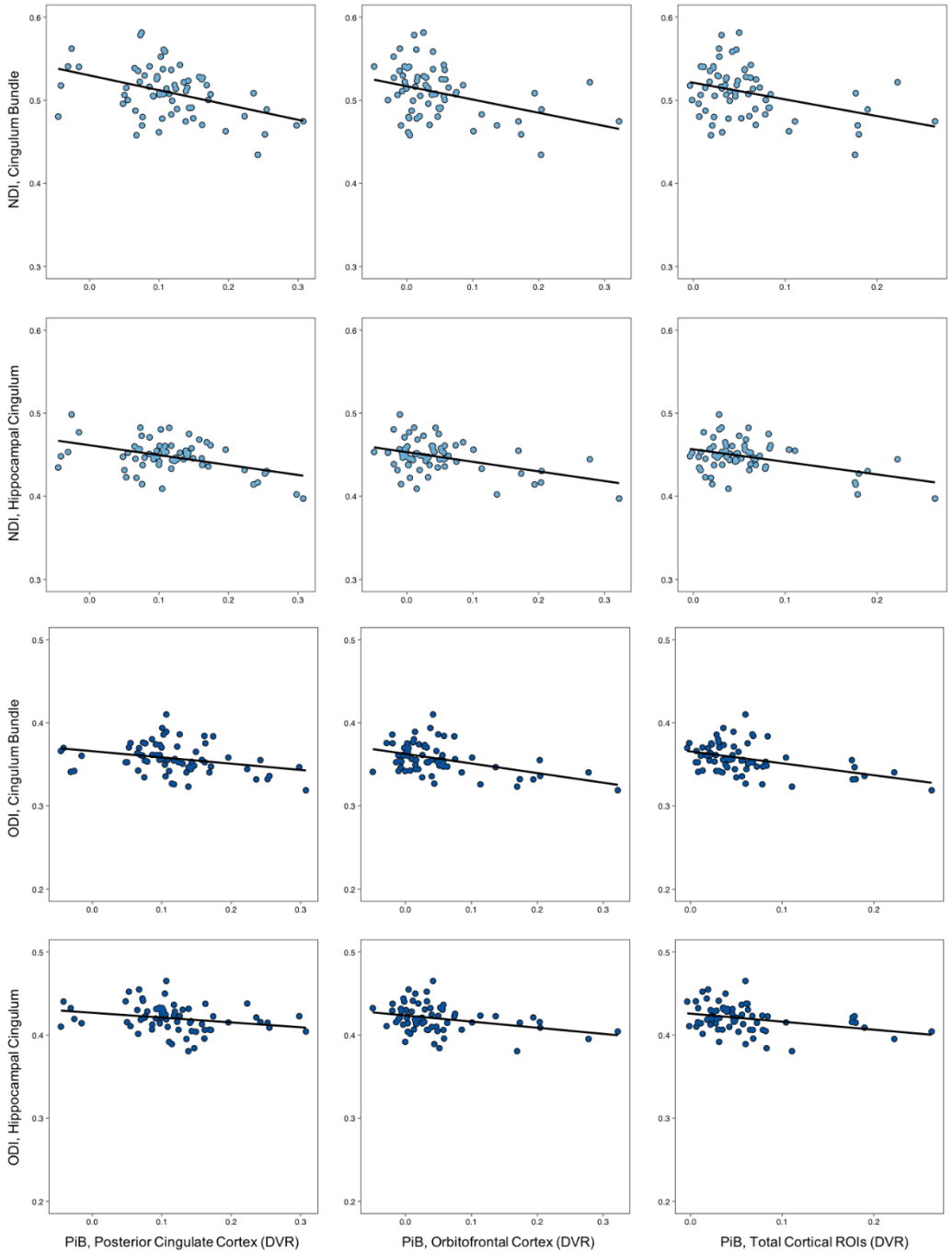

Figure 3: Scatterplots of significant associations between CSF biomarkers and neurite density (NDI, light blue) and orientation dispersion (ODI, dark blue) in the hippocampal cingulum and cingulum ROIs.

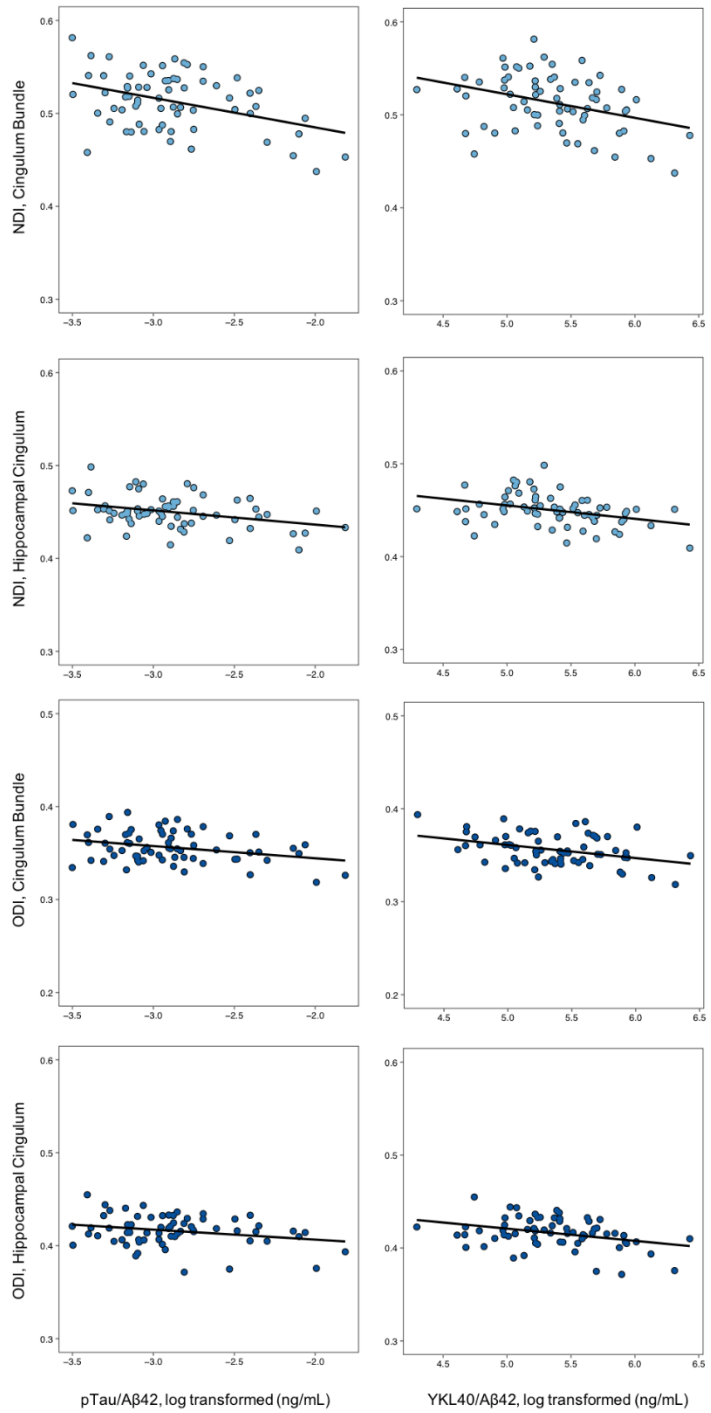

CHAPTER 4

Differential Effects of Neurodegeneration Biomarkers on Subclinical Cognitive Decline

Differential Effects of Neurodegeneration Biomarkers on Subclinical Cognitive Decline

Andrew P. Merluzzi, BA; Nicholas Vogt, BA; Derek Norton, MS; Erin Jonaitis, PhD, MS; Lindsay Clark, PhD; Cynthia M. Carlsson, MD; Sterling C. Johnson, PhD; Sanjay Asthana, MD; Kaj Blennow, MD, PhD; Henrik Zetterberg, MD, PhD; Barbara B. Bendlin, PhD

ABSTRACT:

Objective: Neurodegeneration appears to be the biological mechanism most proximate to cognitive decline in Alzheimer's disease. Yet current indices of neurodegeneration – including total tau in cerebrospinal fluid (CSF) – have yet to undergo comprehensive empirical testing compared to other biomarkers. Here, we test whether t-tau and two alternative biomarkers of neurodegeneration – neurogranin (NG) and neurofilament light protein (NFL) – add value in predicting cognitive decline before the onset of clinical dementia.

Methods: 150 cognitively unimpaired participants received a lumbar puncture for CSF and at least two neuropsychological exams (mean age at first visit = 59.3 ± 6.3 years; 67% female; median number of visits = 3). Linear mixed effects models were used, where the preclinical Alzheimer's consortium composite (PACC), and composite scores for memory, learning, and executive function were used as outcomes. Fixed effects included sex, *APOE* ε4 positivity, a reading score as a proxy for educational and intellectual attainment, age, amyloid positivity (Aβ42/Aβ40 < 0.09), phosphorylated tau positivity (p-tau > 59.50 pg/mL), age*amyloid+, age*p-tau+, and interaction terms of interest: age*NFL or age*NG or age*t-tau. All models included random effects of intercept and slope nested within subject. Nested models with and without the interaction term of interest were compared using likelihood ratio tests and the Akaike information criterion (AIC).

Results: Likelihood ratio tests indicated that age*NFL accounted for a significant amount of variation in longitudinal change on PACC scores ($\chi^2(1) = 26.9$, $\beta = -0.021$, $p < 0.001$), memory composite scores ($\chi^2(1) = 7.8$, $\beta = -0.016$, $p = 0.005$), and learning scores ($\chi^2(1) = 5.89$, $\beta = -0.011$, $p = 0.015$), whereas age*NG and age*t-tau did not. No age by biomarker interactions were statistically significant for the executive function composite score.

Conclusion: These data suggest that NFL may be more sensitive to subclinical cognitive decline compared to other proposed biomarkers for neurodegeneration.

INTRODUCTION

Establishing biomarkers that are predictive of cognitive decline before the onset of dementia is expected to facilitate early intervention in AD. Recently, the amyloid, tau, and neurodegeneration [AT(N)] research framework has been proposed as a biologically-based method for classifying individuals into varying risk categories[159]. In doing so, the aim is to use biomarker status to predict rate of cognitive decline and onset of dementia symptoms[160]. However, it is not yet clear which combination of biomarkers lends the greatest predictive value.

In the current AT(N) framework, is is proposed that amyloidosis can be measured with cerebrospinal fluid (CSF) biomarkers Aβ42 or Aβ42/Aβ40, neurofibrillary tangles with phosphorylated tau (p-tau), and neurodegeneration with total tau (t-tau)[159]. Yet this framework will continue to undergo refinements as new biomarkers are discovered and tested. Indeed, a recently-published framework from the National Institute on Aging – Alzheimer's Association (NIA-AA) suggested that other biomarkers of neurodegeneration – including neurofilament light protein (NFL) and neurogranin (NG) – should be investigated for potential added value in predicting cognitive decline[160].

NFL is a key cytoarchitectural protein present primarily in large-caliber myelinated axons[38]. As such, increased NFL in CSF suggests degeneration or damage of these axons. NG, on the other hand, is expressed within dendritic spines on post-synaptic neurons and plays a key role in plasticity, synapse repair, and long-term potentiation[53]. Increased concentrations of CSF NG signify a loss of synaptic integrity[51, 54, 115].

A small number of studies have compared these biomarkers across disease groups [Merluzzi et al., 2018 *Neurology*] as well as examined their diagnostic accuracy[59, 110, 161]. Other research has investigated their relationships with longitudinal amyloid accumulation, structural brain changes, cognition, and brain metabolism in older populations of participants with varying diagnoses (e.g. cognitively unimpaired, mild cognitive impairment [MCI], and AD-dementia)[110, 162]. Yet less is known about the specific role these biomarkers play in predicting longitudinal, subclinical cognitive decline in younger populations. This is the major goal of the current study. Our primary hypothesis is that NFL and NG will be independently associated with subclinical cognitive decline, and that they will provide additional predictive value compared to t-tau.

METHODS

Participants

Demographic characteristics and biomarker levels for all participants are available in Table 1. 150 Participants (67% female) were recruited from the Wisconsin Registry for Alzheimer's Prevention (WRAP)[130]. This observational cohort consists of participants who were cognitively unimpaired at baseline and middle-aged, with and without parents with AD. All participants are community dwelling, and underwent examination (including lumbar puncture for research purposes) at the University of Wisconsin – Madison. Lumbar punctures were performed between 2009-2014, and neuropsycholgical exams were performed between 2005-2017. The current sample was enriched for AD risk via a parental history of AD (N = 108; 72%) and included some participants positive for the

known AD genetic risk factor *apolipoprotein E* ε4 (*APOE* ε4) (N = 56; 37%). Participants with dementia or MCI were excluded from this study.

Standard Protocol Approvals, Registrations, and Patient Consents

The University of Wisconsin's institutional review board approved all portions of this study and each participant provided written informed consent before all procedures.

Cerebrospinal Fluid Analyses

CSF biomarker collection, assays, and post-processing analysis to account for batch-to-batch variation have been described previously[104, 107, 144]. We measured $A\beta_{42}$, $A\beta_{40}$, and tau phosphorylated at threonine 181 (p-tau), biomarkers that distinguish patients with dementia due to AD from controls[108] and are indicative of conversion from mild cognitive impairment to dementia[109]. In addition to these AD biomarkers, we examined markers of neurodegeneration: t-tau, NFL, and NG. These biomarkers have been associated with cognitive decline in MCI and are elevated in AD patients compared to controls[110]. To measure global amyloidosis, we conducted analyses using $A\beta_{42}/A\beta_{40}$ (rather than $A\beta_{42}$ alone) given that it is more closely associated with amyloid plaque burden measured with molecular brain imaging[111].

Cognitive Composite Scores

To reduce measurement errors, improve the longitudinal stability of cognitive outcomes, and reduce Type 1 errors associated with multiple comparisons, composite scores were computed for learning, memory, and executive function domains, as well as the preclinical Alzheimer's consortium composite (PACC)[163]. Composite scores were created by computing z-scores from raw scores using the population means and standard

deviations for each constituent test. Then, the z-scores within each cognitive domain were averaged to produce the final composite. The tests falling into each composite are as follows:

PACC: Rey Auditory Verbal Learning Test (RAVLT)[164] total trials 1-5, WMS-R LM delayed recall[165], Wechsler Abbreviated Intelligence Scale-Revised (WAIS-R)[166] Digit Symbol Coding total items completed in 90 seconds, and the Mini-Mental State Examination (MMSE)[167]. This composite differs slightly from the originally-proposed composite[163], which includes the total recall score from the Free and Cued Selective Reminding Test (FCSRT)[168] rather than the RAVLT.

Learning: Rey Auditory Verbal Learning Test (RAVLT)[164] total trials 1-5, Wechsler Memory Scale-Revised Logical Memory subtest (WMS-R LM)[165] immediate recall, and the Brief Visuospatial Memory Test (BVMT-R) immediate recall [169].

Memory: RAVLT long-delay free recall[164], WMS-R LM delayed recall[165], and the BVMT-R delayed recall.

Executive functioning: Trail Making Test Part B (TMT B)[170] total time to completion, Stroop Neuropsychological Screening Test color-word interference total items completed in 120 seconds[171], and the Wechsler Abbreviated Intelligence Scale-Revised (WAIS-R)[166] Digit Symbol Coding total items completed in 90 seconds. Because higher raw scores on the TMT B are indicative of poorer performance, the z-score for this test was reversed so that higher composite scores were indicative of better performance.

Statistical Analyses

Pearson correlations were performed between biomarkers for descriptive purposes. For primary analyses, linear mixed effects models were used within the R lme4 package[172], where the PACC and composite scores for memory, executive function, learning were used as separate outcomes[104]. Fixed effects included sex, *APOE* ε4 positivity, WRAT reading score, age at each cognitive visit (centered around the mean baseline visit of the sample), age difference in years between the single time-point LP and each cognitive testing session, amyloid positivity (Aβ42/Aβ40 ≤ 0.09)[173], phosphorylated tau positivity (p-tau ≥ 59.50 pg/mL)[173], age*amyloid positivity, age*p-tau positivity. In addition to these covariates, each model included one of the following terms of interest and its interaction with age: NFL or NG or t-tau (variables were standardized prior to statistical analysis). All models included random effects of intercept and slope nested within subject. In all analyses, a reading score was included as a covariate to control for overall educational and intellectual attainment: the Wide Range Achievement Test (WRAT) 3rd Edition reading subtest[174]. Nested models with and without the interaction term of interest were compared using the Akaike information criterion (AIC) and likelihood ratio tests. Statistical significance was inferred at a family-wise alpha of 0.05, and a Bonferroni correction was applied for the three primary models tested within each cognitive composite (final p = 0.017). Variance inflation factors (VIFs) were examined to assess for model multicollinearity.

Data Availability

For purposes of replicating procedures and results, the data used in this study can be made available upon request.

RESULTS

Pearson correlations between biomarkers are displayed in Table 2. Summary statistics for the PACC, memory, and learning composite models are displayed in Table 3 and statistics for the executive function model are displayed in Table 4. Plots for the PACC, memory composite, and learning composite are in Figures 1, 2, and 3, respectively (while linear mixed effects analyses were performed across all participants regardless of biomarker status, figures 1-3 display results for biomarker negative and biomarker positive groups for illustrative purposes).

Likelihood ratio tests indicated that age*NFL accounted for a significant amount of variation in longitudinal change on PACC scores ($\chi^2(1) = 26.9$, $\beta = -0.021$, $p < 0.001$), whereas age*NG ($\chi^2(1) = 0.001$, $\beta = 0.0002$, $p = 0.96$) and age*t-tau ($\chi^2(1) = 0.0004$, $\beta = 0.0001$, $p = 0.99$) did not. As seen in Table 3, the full NFL model (including the age*NFL interaction) had the lowest AIC of all PACC models.

Likelihood ratio tests indicated that age*NFL also accounted for a significant amount of variation in longitudinal change on the memory composite ($\chi^2(1) = 7.8$, $\beta = -0.016$, $p = 0.005$), whereas age*NG ($\chi^2(1) = 0.74$, $\beta = 0.006$, $p = 0.39$) and age*t-tau ($\chi^2(1) = 0.59$, $\beta = 0.006$, $p = 0.44$) did not. As seen in Table 3, the full NFL model (including the age*NFL interaction) had the lowest AIC of all memory composite models.

Likelihood ratio tests indicated that age*NFL also accounted for a significant amount of variation in longitudinal change on the learning composite ($\chi^2(1) = 5.89$, $\beta = -0.011$, $p = 0.015$), whereas age*NG ($\chi^2(1) = 0.67$, $\beta = 0.004$, $p = 0.42$) and age*t-tau

($\chi^2(1) = 0.41$, $\beta = 0.004$, $p = 0.52$) did not. As seen in Table 3, the full NFL model (including the age*NFL interaction) had the lowest AIC of all learning composite models.

No biomarker interaction terms (age*NFL, age*NG, age*t-tau) were significant for the executive function composite (Table 4). Multicollinearity was not a significant issue in any model (all VIFs < 3).

DISCUSSION

The AT(N) research framework aims to create a biologically-based definition of Alzheimer's disease, and to classify individuals based on etiology and risk of future cognitive decline[159]. However, it is not clear which specific biomarkers will produce the greatest value in predicting cognitive decline before the onset of dementia. Here, we demonstrate that – in a cognitively unimpaired, late middle-aged cohort of individuals at risk for AD – higher levels of NFL are associated with cognitive decline on the PACC as well as learning and memory cognitive composites after accounting for amyloid and p-tau. Further, NFL exhibits stronger associations with cognitive outcomes compared to NG or t-tau.

While the currently-proposed AT(N) framework includes t-tau as a biomarker for neurodegeneration, the utility of this measure in the context of AD remains unclear. It is typically correlated with p-tau, making it difficult to draw conclusions about its independent influence or to build robust statistical models including both of these biomarkers[160, 175]; indeed, in this sample, the Pearson correlation between p-tau and t-tau is 0.80 (see table 2 for full CSF biomarker correlation matrix). Still, as mentioned in the results section, multicollinearity diagnostics were normal for all models herein. The

fact that t-tau produced no additional predictive value above and beyond amyloid and p-tau in the current study underscores the need for more research on additional biomarkers for predicting cognitive decline.

The lack of robust findings for NG was unexpected, as synaptic degeneration is thought to impact the progression from healthy cognition to dementia and may be predictive of neuronal loss[5, 54, 115]. In a cross-sectional study of 132 cognitively unimpaired participants from the WRAP and Wisconsin ADRC cohorts, NG was associated with poorer performance on the RAVLT delayed recall test[176]. Yet, there was no similar relationship found longitudinally for the composite memory score tested here. One possibility is that changes in cognitive composites may be more difficult to detect but therefore more robust when detected. In longitudinal studies, NG has been observed to predict conversion from MCI to frank AD dementia, raising the possibility that increased NG is a robust predictor of cognitive decline only later in the disease course[177, 178]. In partial support of this hypothesis, NG has also been associated with longitudinal cognitive decline, but only in amyloid positive individuals[110]. Similarly, NG has been shown to be associated with regional brain atrophy only in amyloid positive participants[179]. It is possible that the relationship between NG and cognitive decline is insufficiently robust to be measurable early in the disease, or that elevated NG is an important factor only among individuals who have accumulated measurable AD neuropathology burden.

Yet the literature examining differences in biomarkers across neurodegenerative diseases suggest other interpretations for the lack of t-tau and NG

findings in the current study. While t-tau has been considered a marker of gross neurodegeneration and axonal atrophy, some observations do not fit with this interpretation. For example, t-tau elevations appear to be relatively specific to AD; t-tau concentrations are typically lower in patients with other neurodegenerative diseases, such as Parkinson's disease dementia, Lewy-body dementia, and progressive supranuclear palsy[180-184]. With respect to NG, it is important to note that it is not entirely clear what this biomarker represents. If NG was a specific marker for synaptic degeneration, one would expect elevated levels in other neurodegenerative dementias; yet similar to CSF tau, CSF NG elevation is strikingly AD-specific and may in fact be linked to amyloid-related synaptic damage[61, 185].

An alternative interpretation, therefore, is that these biomarkers are specific to AD pathophysiology; that is, rather than reflecting overall neurodegeneration, CSF tau and NG are excreted from neurons in an AD-specific process, whereby tau undergoes hyperphosphorylation and neurons truncate and subsequently secrete t-tau, p-tau, and NG[153]. Neurofibrillary tangle development, compromised axonal transport, and degeneration may then occur in these affected neurons, which would follow the elevated concentrations of t-tau, p-tau, and NG detectable in CSF. This interpretation of CSF tau is supported by both animal and human data: Maia *et al*. found an Aβ-dependent increase in tau secretion into CSF in APP-transgenic mice in the absence of neurodegeneration[186]. In addition, stable isotope labeling experiments in humans revealed increased tau secretion into CSF in Aβ-positive cases[187]. To the best of our knowledge, similar data for NG do not yet exist.

Interpretations are more straightforward for NFL as a marker of neurodegeneration. NFL is present in large-caliber myelinated axons connecting temporal and frontal lobes,[38, 49] and is a crucial component of the neuronal cytoskeleton[40, 41] It is robustly elevated in many neurodegenerative diseases[49], appears to be relatively independent of amyloid and tau levels,[48, 110, 179] and correlates with symptomology, progression, and survival[48, 113]. NFL may be an especially promising biomarker for neurodegeneration because it may be measurable in plasma[113]. Further, because NFL was associated with cognitive decline while controlling for Aβ42/Aβ40 and p-tau in the current study, it may be useful as a predictive biomarker independent of obvious AD neuropathology.

There are several limitations of the current study that deserve note. First, while CSF $A\beta_{42}/A\beta_{40}$ and p-tau are widely-used metrics of AD neuropathology, they do not capture regional variation in the deposition of amyloid and tau that may play a crucial role in predicting cognitive decline[188]. Studies using amyloid and tau positron emission tomography (PET) will be invaluable for determining whether regional protein accumulation does in fact add value in predicting cognitive decline before the onset of dementia. In addition, generalizability to other populations may be difficult: the vast majority of this sample is Caucasian and highly educated. Intensive recruitment of underrepresented populations is currently underway.

It is also worth noting the lack of amyloid-related cognitive decline in this study. Other studies have demonstrated that beta-amyloid deposition is associated with cognitive decline[189-193], including on individual cognitive tests[194], and on cognitive

composite scores[104]. Many of the previous studies had larger sample sizes than the current study, and examined relationships between different independent variables (CSF versus PiB-PET) with different dependent variables (individual cognitive tests versus composite scores). Clearly, more work will be required to understand the independent effect of amyloid on cognitive decline, and whether specific neurodegenerative processes (like axonal degeneration) mediate this relationship.

While the results of this study provide data that may guide selection of markers within the AT(N) framework, other modalities are also expected to show utility. [^{18}F]fluorodeoxyglucose positron emission tomography (FDG-PET) and structural magnetic resonance imaging are common methods of indexing neurodegenerative processes[160], and additional sensitive brain imaging metrics are undergoing testing and development – including synaptic vesicle glycoprotein 2A for indexing synaptic density[195]. Ultimately, research comparing the utility of each of these techniques will be crucial for creating a valid, biologically-based definition of AD etiology and risk of cognitive decline.

While continuous variables are useful for describing biological phenomena from a research perspective, cut points may ultimately be more useful for bringing research results into clinical care. Because the AT(N) framework aims to categorize individuals based on biomarker status, an important next step in this research will be to create clinically-relevant cut points for neurodegeneration biomarkers, including NFL. To that end, it will be crucial to follow these participants longitudinally to determine whether NFL

is also predictive of faster decline to MCI or dementia, rather than the subclinical decline measured here.

CONCLUSION

The data presented here suggest that NFL may lend additional value to the AT(N) framework, and that it may be more sensitive in detecting cognitive decline before the onset of dementia than either t-tau or NG. Our findings underscore the idea that axonal degeneration may play an important role in cognitive decline before the onset of dementia due to AD – or perhaps independent of AD, given that NFL was associated with cognitive decline independently of Aβ and p-tau neuropathology. This study also calls for more research on how t-tau, NG, NFL and other neurodegeneration biomarkers contribute to the pathogenesis of Alzheimer's disease.

Funding:

This project was supported by NIH grants AG037639 (BBB), AG027161 (SCJ), P50 AG033514 (SA), AG054059 (PI Carey Gleason, PhD), the UW Institute for Clinical and Translation Research grant 1UL1RR025011, the Geriatric Research, Education, and Clinical Center (GRECC) of the William S. Middleton Memorial Veterans Hospital, the Swedish Alzheimer Foundation (# AF-553101 and AF-646211), the Torsten Söderberg Foundation (KB), the Research Council of Sweden (project #14002) (KB), the Swedish Brain Foundation (project # FO2015-0021) (KB), LUA/ALF Västra Götalandsregionen (VGR) Sweden (project # ALFGBG-139671) (KB), the European Research Council (#681712) (HZ), Swedish State Support for Clinical Research (#ALFGBG-441051) (HZ), the Knut and Alice Wallenberg Foundation (Wallenberg

Academy Fellow 2013) (HZ), and the National Science Foundation Graduate Research Fellowship under Grant No. DGE-1256259 (APM). Any opinions, findings, and conclusions or recommendations expressed in this material are those of the authors(s) and do not necessarily reflect the views of the National Science Foundation.

Tables and Figures

Table 1: Table 1: Participant characteristics. Values are mean (standard deviation) except where otherwise indicated.

Sample Characteristics	**Total**
2 Cognitive Visits, N (% of sample)	150 (100%)
3 Cognitive Visits, N (% of sample)	141 (94%)
4 Cognitive Visits, N (% of sample)	101 (67%)
5 Cognitive Visits, N (% of sample)	17 (11%)
Age at Baseline Cognitive Visit, Years	59.3 (6.3)
Age at LP, Years	61.0 (6.5)
Age Difference Between LP and Cognitive Visits, Years	1.7 (2.9)
Female, N (% Female)	101 (67%)
Parental History of AD, N (% Positive)	108 (72%)
APOE ε4, N (% Positive)	56 (37%)
WRAT-3 Reading Subtest Raw Score	51.6 (4.3)
MMSE	29.3 (0.9)
NFL, pg/mL	676 (350)
Neurogranin, pg/mL	388 (176)
Aβ42/Aβ40	0.09 (0.02)
P-tau, pg/mL	47 (18)
T-tau, pg/mL	325 (125)
Amyloid Positive, N (% of sample)	46 (31%)
P-tau Positive, N (% of sample)	20 (13%)
Amyloid and P-tau Positive, N (% of sample)	9 (6%)

Abbreviations: LP, Lumbar Puncture; AD, Alzheimer's disease; APOE4, apolipoprotein E gene ε4; WRAT, Wide Range Achievement Test; MMSE, mini-mental state examination; NFL, neurofilament light protein; Aβ42/Aβ40, amyloid beta 42 and amyloid beta 40 peptide ratio; p-tau, tau phosphorylated at threonine 181; t-tau, total tau

Table 2: Pearson correlation matrix between biomarkers used in the current study.

	Aβ42/Aβ40	P-tau	T-tau	Neurogranin	NFL
Aβ42/Aβ40	1				
P-tau	-0.14	1			
T-tau	-0.31	0.80	1		
Neurogranin	-0.28	0.64	0.74	1	
NFL	-0.12	0.26	0.32	0.10	1

Abbreviations: NFL, neurofilament light protein; Aβ42/Aβ40, amyloid beta 42 and amyloid beta 40 peptide ratio; p-tau, tau phosphorylated at threonine 181; t-Tau, total tau

Table 3: Statistical summary of the preclinical Alzheimer's consortium composite (PACC), memory composite, and learning composite models, including beta coefficients and standard errors.

Linear Mixed Effects Models									
	PACC			Memory Composite			Learning Composite		
	T-tau	NG	NFL	T-tau	NG	NFL	T-tau	NG	NFL
Age (Centered)	-0.031***	-0.031***	-0.032***	-0.030**	-0.029**	-0.032***	-0.025***	-0.024***	-0.027***
	(0.006)	(0.007)	(0.006)	(0.009)	(0.009)	(0.009)	(0.007)	(0.007)	(0.007)
Sex	0.158*	0.153*	0.143*	0.356***	0.344***	0.344***	0.188*	0.179*	0.186*
	(0.070)	(0.070)	(0.068)	(0.103)	(0.103)	(0.102)	(0.077)	(0.076)	(0.077)
APOE ε4	-0.030	-0.032	-0.031	-0.151	-0.146	-0.142	-0.114	-0.104	-0.104
	(0.070)	(0.071)	(0.069)	(0.103)	(0.104)	(0.102)	(0.078)	(0.078)	(0.077)
WRAT Score	0.040***	0.039***	0.030***	0.056***	0.054***	0.049***	0.039***	0.037***	0.035***
	(0.008)	(0.008)	(0.008)	(0.012)	(0.012)	(0.012)	(0.009)	(0.009)	(0.009)
Age Difference	0.008	0.007	0.003	0.041***	0.041***	0.038***	0.040***	0.040***	0.038***
	(0.007)	(0.007)	(0.007)	(0.009)	(0.009)	(0.009)	(0.007)	(0.007)	(0.007)
Amyloid Positivity	-0.101	-0.075	-0.038	-0.169	-0.101	-0.108	-0.139	-0.079	-0.120
	(0.082)	(0.081)	(0.077)	(0.120)	(0.117)	(0.111)	(0.093)	(0.090)	(0.086)
P-tau Positivity	-0.049	0.0001	0.065	0.041	0.189	0.157	0.078	0.216	0.121
	(0.110)	(0.110)	(0.096)	(0.162)	(0.161)	(0.139)	(0.125)	(0.123)	(0.107)
T-tau	0.044			0.068			0.028		
	(0.041)			(0.060)			(0.046)		
NG		0.009			-0.034			-0.068	
		(0.040)			(0.058)			(0.044)	
NFL			-0.012			0.017			0.040
			(0.041)			(0.059)			(0.046)
Age X Amyloid Positivity	-0.008	-0.008	0.001	-0.012	-0.012	-0.002	-0.006	-0.006	0.001
	(0.009)	(0.009)	(0.008)	(0.013)	(0.013)	(0.012)	(0.010)	(0.010)	(0.009)
Age X P-tau Positivity	-0.018	-0.018	-0.001	-0.052**	-0.052**	-0.032	-0.029	-0.031	-0.015
	(0.014)	(0.014)	(0.012)	(0.020)	(0.020)	(0.017)	(0.016)	(0.016)	(0.014)
Age X T-tau	0.0001			0.006			0.004		
	(0.005)			(0.007)			(0.005)		
Age X NG		0.0002			0.006			0.004	
		(0.005)			(0.007)			(0.005)	
Age X NFL			-0.021***			-0.016**			-0.011*
			(0.004)			(0.006)			(0.005)
Constant	-2.080***	-2.029***	-1.557***	-2.944***	-2.845***	-2.605***	-1.989***	-1.935***	-1.806***
	(0.403)	(0.403)	(0.398)	(0.591)	(0.591)	(0.596)	(0.443)	(0.439)	(0.449)
Observations	559	559	559	559	559	559	559	559	559
AIC	548.5	549.6	511.2	866.8	868.1	860.1	661.8	660.4	656.7

***p < .001; **p < .01; *p < .05

Abbreviations: *APOE* ε4, apolipoprotein E gene ε4; WRAT, Wide Range Achievement Test; Age Difference, years between lumbar puncture and cognitive exams; p-tau, tau phosphorylated at threonine 181; t-tau, total tau; NG, neurogranin; NFL, neurofilament light protein; AIC, Akaike information criterion

Table 4: Statistical summary of the executive function composite models, including beta coefficients and standard errors.

Linear Mixed Effects Models

	Executive Function Composite		
	T-tau	**NG**	**NFL**
Age (Centered)	-0.068***	-0.068***	-0.066***
	(0.008)	(0.008)	(0.008)
Sex	0.072	0.077	0.066
	(0.096)	(0.096)	(0.097)
APOE ε4	0.148	0.149	0.144
	(0.095)	(0.096)	(0.095)
WRAT Score	0.037***	0.038***	0.035**
	(0.011)	(0.011)	(0.011)
Age Difference	0.029***	0.030***	0.028***
	(0.008)	(0.008)	(0.008)
Amyloid Positivity	-0.033	-0.057	-0.046
	(0.108)	(0.106)	(0.102)
P-tau Positivity	0.012	-0.035	-0.018
	(0.149)	(0.148)	(0.131)
T-tau	-0.039		
	(0.055)		
NG		-0.007	
		(0.054)	
NFL			-0.050
			(0.052)
Age X Amyloid Positivity	-0.0002	-0.001	-0.002
	(0.009)	(0.009)	(0.009)
Age X P-tau Positivity	0.005	0.004	0.002
	(0.014)	(0.014)	(0.012)
Age X T-tau	-0.003		
	(0.005)		
Age X NG		-0.002	
		(0.005)	
Age X NFL			-0.0001
			(0.004)
Constant	-1.898***	-1.941***	-1.797**
	(0.541)	(0.541)	(0.552)
Observations	559	559	559
AIC	519.4	520.0	519.2

***p < .001; **p < .01; *p < .05

Abbreviations: *APOE* ε4, apolipoprotein E gene ε4; WRAT, Wide Range Achievement Test; Age Difference, years between lumbar puncture and cognitive exams; p-tau, tau phosphorylated at threonine 181; t-tau, total tau; NG, neurogranin; NFL, neurofilament light protein; AIC, Akaike information criterion

Figure 1: Linear relationships between age (centered on the sample mean), Alzheimer's biomarker status, and standardized cognitive scores on the preclinical Alzheimer's consortium composite (PACC), adjusted for covariates. The top row represents individuals positive for both amyloid and p-tau pathology, whereas the bottom row represents individuals negative on these biomarkers. While linear mixed effects analyses were performed across all participants regardless of biomarker status, results for biomarker negative and biomarker positive groups are displayed here for illustrative purposes. Blue represents the highest quartile of t-tau, neurogranin, and NFL, and red the lowest quartile. Higher NFL, but not t-tau or neurogranin, was associated with longitudinal cognitive decline independent of amyloid and p-tau concentrations.

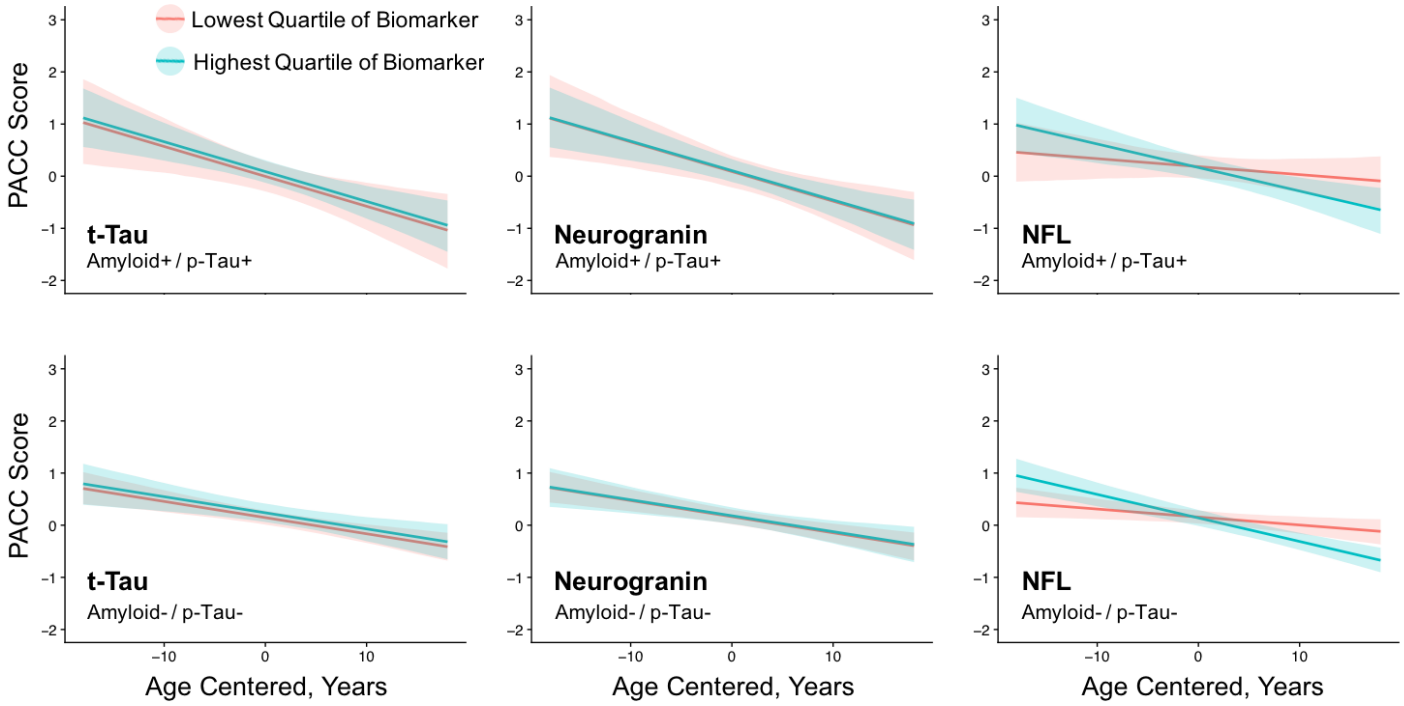

Figure 2: Linear relationships between age (centered on the sample mean), Alzheimer's biomarker status, and standardized scores on the memory composite, adjusted for covariates. The top row represents individuals positive for both amyloid and p-tau pathology, whereas the bottom row represents individuals negative on these biomarkers. While linear mixed effects analyses were performed across all participants regardless of biomarker status, results for biomarker negative and biomarker positive groups are displayed here for illustrative purposes. Blue represents the highest quartile of t-tau, neurogranin, and NFL, and red the lowest quartile. Higher NFL, but not t-tau or neurogranin, was associated with longitudinal cognitive decline independent of amyloid and p-tau concentrations.

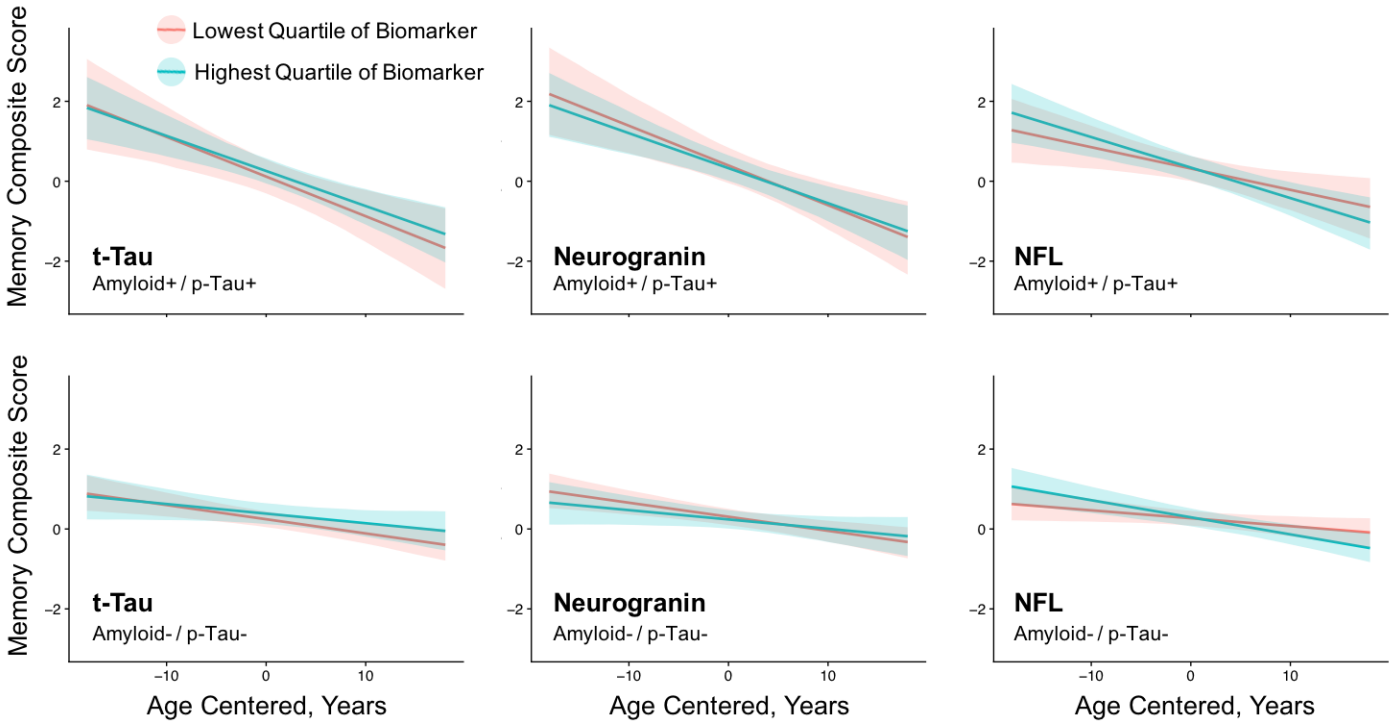

Figure 3: Linear relationships between age (centered on the sample mean), Alzheimer's biomarker status, and standardized scores on the learning composite, adjusted for covariates. The top row represents individuals positive for both amyloid and p-tau pathology, whereas the bottom row represents individuals negative on these biomarkers. While linear mixed effects analyses were performed across all participants regardless of biomarker status, results for biomarker negative and biomarker positive groups are displayed here for illustrative purposes. Blue represents the highest quartile of t-tau, neurogranin, and NFL, and red the lowest quartile. Higher NFL, but not t-tau or neurogranin, was associated with longitudinal cognitive decline independent of amyloid and p-tau concentrations.

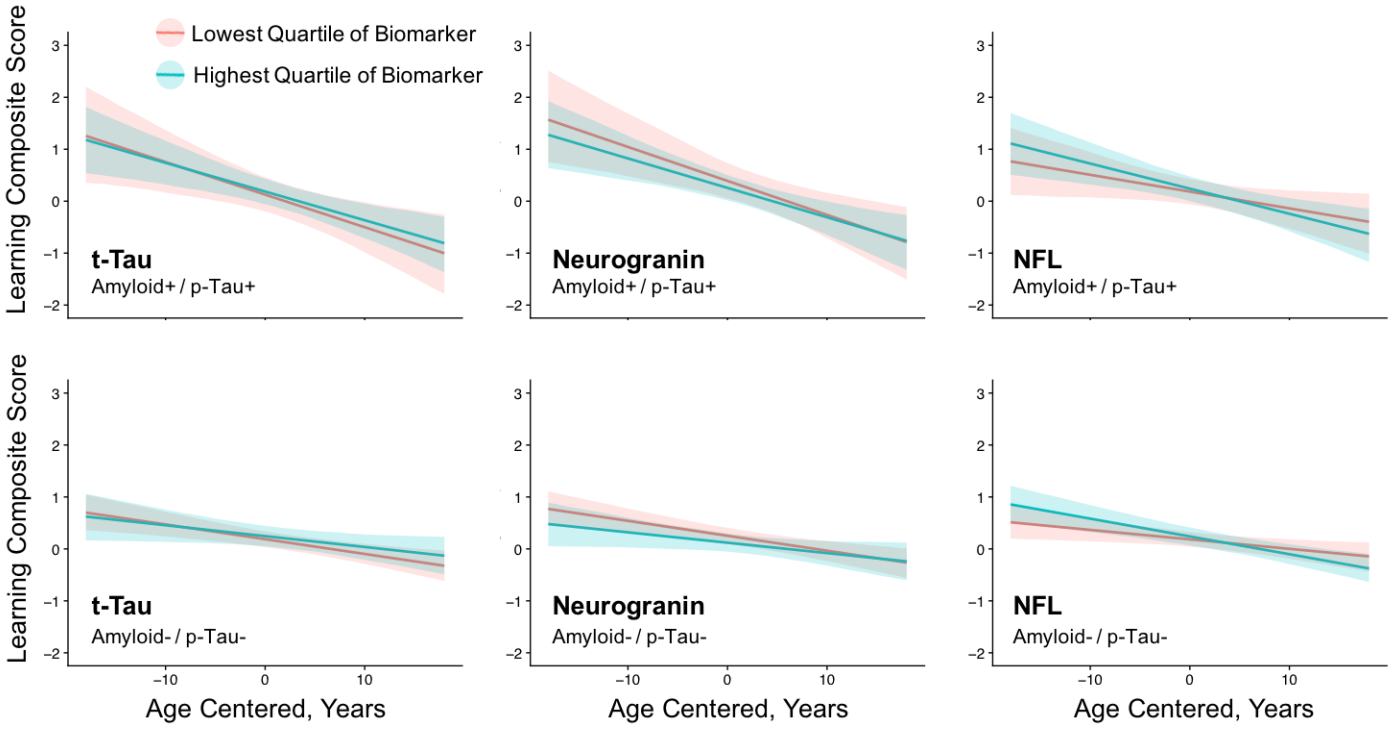

CHAPTER 5

Conclusions and Future Directions

The preclinical stage of Alzheimer's disease is characterized by the accumulation of AD neuropathology (Aβ and NFT) without significant cognitive impairments. Indeed, post-mortem studies have shown that many individuals with significant Aβ and NFT pathology did not exhibit dementia during life – these people, had they lived longer, were perhaps in the preclinical stage of AD[27]. Importantly, those with dementia, on the other hand, also exhibited other pathologies, including neural injury and gliosis. This evidence was a primary motivator of the research presented here, which focuses on understanding the biological processes co-occurring with amyloid and NFT accumulation during asymptomatic stages of the disease (i.e. the preclinical stage).

From the standpoint of intervention, the preclinical stage is perhaps a "sensitive period" for altering the disease course[160]. Yet, to design truly effective interventions, more knowledge is needed about the biological processes occurring early in the disease course. This dissertation sheds light on these processes, and provides evidence that neural injury, synaptic dysfunction, and gliosis may play important roles before the onset of dementia.

Aim 1 demonstrated that cognitively unimpaired individuals with significant AD neuropathology tend to have lower levels of neural injury (NFL, t-tau) and gliosis (YKL-40) biomarkers than those with similar AD neuropathology and a clinical diagnosis of dementia. As explained below, these Mismatch individuals may be in the preclinical stage.

Aim 2 revealed a link between amyloid (measured with PiB-PET) and white matter microstructure, but argues against the notion that amyloid itself is locally toxic to

the neurons comprising adjacent white matter tracts. Additionally, this study demonstrated that p-tau/$A\beta_{42}$ and YKL-40/$A\beta_{42}$ are associated with alterations in white matter microstructure in similar tracts, suggesting that p-tau accumulation or gliosis may be driving factors toward alterations in brain microstructure.

Finally, the findings from Aim 3 suggest that axonal degeneration – as indexed by NFL – may prove to be an important biological factor leading to cognitive decline, perhaps more so than the processes of synaptic degeneration and gross neurodegeneration that NG and t-tau are thought to measure.

Future Directions

There are several important future research directions for the studies presented here. For Aim 1, a crucial next step will be to determine whether the Mismatch individuals do undergo cognitive decline, and if so how steep this decline is. This will be difficult to measure with the current study sample, as there were only a small number of Mismatch individuals in the age-matched analysis. However, by using the methodology described in Chapter 2 and combining across centers collecting similar data, it may be possible to determine whether elevations in YKL-40, NFL, t-tau, or NG are immediate precursors to cognitive decline.

Indeed, the neurogranin results presented in Aim 1 do point toward this outcome. Whereas neurogranin exhibited low signal in predicting outcomes in Aim 2 and Aim 3, the fact that Mismatches had comparable levels to the AD-Dementia group in Aim 1 provides support for the idea that significant neurodegeneration is occurring in Mismatches, and that cognitive decline may be imminent. Neurogranin itself has been

implicated in the progression from MCI to dementia, but may in fact be less predictive of the progression from normal cognition to MCI[177, 178].

There are other crucial studies required to advance the Aim 1 findings. It will be important to understand what other lifestyle factors contribute to resilience in the face of significant AD neuropathology burden, and whether the "resilience" in this case connotes prevention or simply delay to cognitive decline. While years of education may be a reasonable proxy for other metrics, there are almost certainly crucial latent variables that require exploration (e.g. quality of education, occupational complexity[196], social factors contributing to cognitive reserve[197]. Diet, exercise, and cognitive engagement have all been put forth as possible modifiable risk factors[198]. If such results prove promising, there are of course still broader policy problems in designing incentives that increase healthy behaviors and decrease risk.

With respect to the neurobiology findings presented in Aim 2, more research is needed to determine the relationship between Aβ and white matter microstructure. Is there a causative pathway between amyloid deposition and altered white matter microstructure? If not, as Aim 2 suggests, other variables upstream of both phenomena should be investigated. There have been suggestions in the literature that myelin degeneration can initiate amyloid accumulation[199], but also evidence that amyloid can seed NFT, which can then produce Wallerian neurodegeneration in white matter tracts. Neuroanatomically, this latter hypothesis – that unmeasured NFT in Aim 2 leads to altered white matter microstructure – would explain why we observed altered white matter microstructure in the hippocampal cingulum, as early NFT deposition in the

medial temporal lobe could cause cell death and Wallerian degeneration. However, it would be harder to make the case that NFT caused altered white matter microstructure in the cingulum, or why it was not associated with altered microstructure in the uncinate fasciculus. Clearly, more work is needed to untangle the relationship between typical AD neuropathologies and white matter microstructure.

Research is also needed to understand subtle predictive discrepancies between $A\beta_{42}/A\beta_{40}$ and PiB-PET. While the global PiB measure and $A\beta_{42}/A\beta_{40}$ are highly correlated, and show strong relationships over time[132, 200, 201], these two methods of measuring amyloidosis may still be contributing unique information, particular at different stages in the disease[202]. It is possible that, by the time Aβ deposition has increased enough to be detectable in the brain with PET imaging, there are already white matter alterations occurring – perhaps altogether independent of Aβ deposition. Because amyloidosis is thought to be more readily detectable at earlier stages in CSF[202] on the other hand, high concentrations of $A\beta_{42}/A\beta_{40}$ may in fact precede significant white matter changes. An important caveat with respect to Aim 2 is that the PiB and CSF analyses were not conducted in exactly the same participants. While 52 of the participants in Aim 2 were included in both the PiB and CSF analyses, this left 16 and 17 participants independent in each analysis. It is possible these other participants account for the discrepancy between the CSF and PET findings.

The evidence in Aim 3 broadly suggests that more research is needed on novel biomarkers that provide additional value in predicting cognitive decline. It is possible that, in similar designs to the ones presented in Aim 3, other biomarkers of

neurodegeneration (e.g. SNAP-25, VILIP-1, synaptotagmin) will provide more value than t-tau, NG, or NFL[203].

It is also likely that the AT(N) model itself fails to capture the complex heterogeneity present in AD pathophysiology. Many studies have pointed to the important role that vascular pathology plays in the development of AD[204, 205]. Further, there is clearly an important role for innate immunity and inflammation in the pathogenesis of the disease – Aim 1 demonstrated that YKL-40 may be useful in differentiating Mismatch from AD-Dementia, and perhaps other, more specific markers of gliosis will prove valuable in predicting cognitive decline[36].

In addition to adding longitudinal analyses and investigating novel CSF biomarkers, the studies presented here and AD research in general will benefit from new molecular imaging targets. PET tracers for NFT are currently under development, and early results from a new tracer, MK-6240, suggest high specificity with little off-target[206]. Other tracers, such as SV2A for quantifying synaptic density[207], as well as PBR28 for quantifying microglia concentrations[208], hold promise for increasing our understanding of auxiliary biological processes occurring at all stages of the disease. Ultimately, multi-modal investigations will prove most useful in understanding the many facets of AD. In conjunction with the biomarker work in living humans, post-mortem research will be invaluable for validating *in vivo* results.

From a research design perspective, the field should focus more intently on recruiting participants from underrepresented backgrounds. In all three Aims of this dissertation, the vast majority of participants were Caucasian and highly educated.

Given the stark disparities in Alzheimer's incidence and outcomes[209, 210], it is important to understand how the disease manifests in diverse populations, as well as how other risk factors associated with underrepresented groups contribute to the biology of dementia[211]. It is possible, for instance, that the AT(N) framework is inadequate for capturing the idiosyncrasies of underrepresented populations, and that including other risk factors (such as vascular disease) would add value in predicting cognitive decline.

Recruiting underrepresented groups into research programs will also prove useful for determining the population compositions for future clinical trials. It may be the case that drug targets useful for Caucasian participants do not readily map on to African Americans, or vice versa. While this is an area in which more research is needed, the results presented in this dissertation point to several avenues by which biomarkers might be useful for informing clinical trial recruitment. For instance, participants with high AD neuropathology burden but low NFL, YKL-40, NG, or white matter microstructural pathology might be the population most amenable to drug trial interventions.

In sum, this research adds to the growing body of scholarship pointing toward the notion that Aβ and NFT are necessary but not sufficient for the onset of clinical dementia. Further, these studies provide evidence that measuring several other biological processes (e.g. neural injury, white matter microstructure, synaptic degeneration, and gliosis) may lend additional insight into the pathogenesis of AD.

REFERENCES:

1. Strassnig M, Ganguli M. About a peculiar disease of the cerebral cortex. By Alois Alzheimer, 1907 (Translated by L. Jarvik and H. Greenson). Alzheimer disease and associated disorders 1907;1:3-8.
2. Goedert M, Spillantini MG. A century of Alzheimer's disease. science 2006;314:777-781.
3. Mangialasche F, Solomon A, Winblad B, Mecocci P, Kivipelto M. Alzheimer's disease: clinical trials and drug development. The Lancet Neurology 2010;9:702-716.
4. Terry RD, Masliah E, Salmon DP, et al. Physical basis of cognitive alterations in Alzheimer's disease: synapse loss is the major correlate of cognitive impairment. Annals of neurology 1991;30:572-580.
5. DeKosky ST, Scheff SW. Synapse loss in frontal cortex biopsies in Alzheimer's disease: correlation with cognitive severity. Annals of neurology 1990;27:457-464.
6. Selkoe DJ. Alzheimer's disease is a synaptic failure. Science 2002;298:789-791.
7. Scheff S, Price D, Schmitt F, DeKosky S, Mufson E. Synaptic alterations in CA1 in mild Alzheimer disease and mild cognitive impairment. Neurology 2007;68:1501-1508.
8. Blennow K, Bogdanovic N, Alafuzoff I, Ekman R, Davidsson P. Synaptic pathology in Alzheimer's disease: relation to severity of dementia, but not to senile plaques, neurofibrillary tangles, or the ApoE4 allele. Journal of neural transmission 1996;103:603-618.
9. Jack CR, Knopman DS, Jagust WJ, et al. Tracking pathophysiological processes in Alzheimer's disease: an updated hypothetical model of dynamic biomarkers. The Lancet Neurology 2013;12:207-216.
10. Hardy J. The amyloid hypothesis for Alzheimer’s disease: a critical reappraisal. Journal of neurochemistry 2009;110:1129-1134.
11. Galasko D. Expanding the repertoire of biomarkers for alzheimer’s disease: targeted and non-targeted approaches. Frontiers in neurology 2015;6.
12. McLellan ME, Kajdasz ST, Hyman BT, Bacskai BJ. In vivo imaging of reactive oxygen species specifically associated with thioflavine S-positive amyloid plaques by multiphoton microscopy. Journal of Neuroscience 2003;23:2212-2217.
13. Ingelsson M, Fukumoto H, Newell K, et al. Early Aβ accumulation and progressive synaptic loss, gliosis, and tangle formation in AD brain. Neurology 2004;62:925-931.
14. Serrano-Pozo A, Mielke ML, Gómez-Isla T, et al. Reactive glia not only associates with plaques but also parallels tangles in Alzheimer's disease. The American journal of pathology 2011;179:1373-1384.
15. Bozzali M, Falini A, Franceschi M, et al. White matter damage in Alzheimer's disease assessed in vivo using diffusion tensor magnetic resonance imaging. Journal of Neurology, Neurosurgery & Psychiatry 2002;72:742-746.
16. Rose SE, Chen F, Chalk JB, et al. Loss of connectivity in Alzheimer's disease: an evaluation of white matter tract integrity with colour coded MR diffusion tensor imaging. J Neurol Neurosurg Psychiatry 2000;69:528-530.
17. Zhang Y, Schuff N, Jahng G-H, et al. Diffusion tensor imaging of cingulum fibers in mild cognitive impairment and Alzheimer disease. Neurology 2007;68:13-19.
18. Melah KE, Lu SY-F, Hoscheidt SM, et al. CSF markers of Alzheimer’s pathology and microglial activation are associated with altered white matter microstructure in asymptomatic adults at risk for Alzheimer’s disease. Journal of Alzheimer's disease: JAD 2016;50:873.

19. Bendlin BB, Carlsson CM, Johnson SC, et al. CSF T-Tau/Aβ 42 Predicts White Matter Microstructure in Healthy Adults at Risk for Alzheimer's Disease. PLoS One 2012;7:e37720.
20. Racine AM, Adluru N, Alexander AL, et al. Associations between white matter microstructure and amyloid burden in preclinical Alzheimer's disease: a multimodal imaging investigation. NeuroImage: Clinical 2014;4:604-614.
21. Adluru N, Destiche DJ, Lu SY-F, et al. White matter microstructure in late middle-age: effects of apolipoprotein E4 and parental family history of Alzheimer's disease. NeuroImage: Clinical 2014;4:730-742.
22. Hardy JA, Higgins GA. Alzheimer's disease: the amyloid cascade hypothesis. Science 1992;256:184.
23. Forlenza OV, Diniz BS, Gattaz WF. Diagnosis and biomarkers of predementia in Alzheimer's disease. BMC medicine 2010;8:89.
24. Sadleir KR, Kandalepas PC, Buggia-Prévot V, Nicholson DA, Thinakaran G, Vassar R. Presynaptic dystrophic neurites surrounding amyloid plaques are sites of microtubule disruption, BACE1 elevation, and increased Aβ generation in Alzheimer's disease. Acta neuropathologica 2016;132:235-256.
25. Olsson F, Schmidt S, Althoff V, et al. Characterization of intermediate steps in amyloid beta (Aβ) production under near-native conditions. Journal of Biological Chemistry 2014;289:1540-1550.
26. Selkoe DJ, Hardy J. The amyloid hypothesis of Alzheimer9s disease at 25 years. EMBO molecular medicine 2016;8:595-608.
27. Perez-Nievas BG, Stein TD, Tai H-C, et al. Dissecting phenotypic traits linked to human resilience to Alzheimer's pathology. Brain 2013:awt171.
28. Katzman R, Aronson M, Fuld P, et al. Development of dementing illnesses in an 80-year-old volunteer cohort. Annals of neurology 1989;25:317-324.
29. Schneider JA, Aggarwal NT, Barnes L, Boyle P, Bennett DA. The neuropathology of older persons with and without dementia from community versus clinic cohorts. Journal of Alzheimer's Disease 2009;18:691-701.
30. Rowe CC, Ng S, Ackermann U, et al. Imaging β-amyloid burden in aging and dementia. Neurology 2007;68:1718-1725.
31. Aizenstein HJ, Nebes RD, Saxton JA, et al. Frequent amyloid deposition without significant cognitive impairment among the elderly. Archives of neurology 2008;65:1509-1517.
32. Stern Y. Cognitive reserve in ageing and Alzheimer's disease. The Lancet Neurology 2012;11:1006-1012.
33. Satz P. Brain reserve capacity on symptom onset after brain injury: A formulation and review of evidence for threshold theory. Neuropsychology 1993;7:273.
34. Davies C, Mann D, Sumpter P, Yates P. A quantitative morphometric analysis of the neuronal and synaptic content of the frontal and temporal cortex in patients with Alzheimer's disease. Journal of the neurological sciences 1987;78:151-164.
35. Bertoni-Freddari C, Fattoretti P, Casoli T, Caselli U, Meier-Ruge W. Deterioration threshold of synaptic morphology in aging and senile dementia of Alzheimer's type. Analytical and quantitative cytology and histology/the International Academy of Cytology [and] American Society of Cytology 1996;18:209-213.
36. Heneka MT, Carson MJ, El Khoury J, et al. Neuroinflammation in Alzheimer's disease. The Lancet Neurology 2015;14:388-405.

37. Jack CR, Wiste HJ, Weigand SD, et al. Age-specific population frequencies of cerebral β-amyloidosis and neurodegeneration among people with normal cognitive function aged 50–89 years: a cross-sectional study. The Lancet Neurology 2014;13:997-1005.
38. Elder GA, Friedrich VL, Bosco P, et al. Absence of the mid-sized neurofilament subunit decreases axonal calibers, levels of light neurofilament (NF-L), and neurofilament content. The Journal of cell biology 1998;141:727-739.
39. Friede RL, Samorajski T. Axon caliber related to neurofilaments and microtubules in sciatic nerve fibers of rats and mice. The Anatomical Record 1970;167:379-387.
40. Petzold A. Neurofilament phosphoforms: surrogate markers for axonal injury, degeneration and loss. Journal of the neurological sciences 2005;233:183-198.
41. Schlaepfer W, Lynch R. Immunofluorescence studies of neurofilaments in the rat and human peripheral and central nervous system. The Journal of cell biology 1977;74:241.
42. Jonsson M, Zetterberg H, Van Straaten E, et al. Cerebrospinal fluid biomarkers of white matter lesions–cross-sectional results from the LADIS study. European journal of neurology 2010;17:377-382.
43. Waldö ML, Santillo AF, Passant U, et al. Cerebrospinal fluid neurofilament light chain protein levels in subtypes of frontotemporal dementia. BMC neurology 2013;13:54.
44. Madeddu R, Farace C, Tolu P, et al. Cytoskeletal proteins in the cerebrospinal fluid as biomarker of multiple sclerosis. Neurological sciences 2013;34:181-186.
45. Jeppsson A, Zetterberg H, Blennow K, Wikkelsø C. Idiopathic normal-pressure hydrocephalus Pathophysiology and diagnosis by CSF biomarkers. Neurology 2013;80:1385-1392.
46. Tortelli R, Ruggieri M, Cortese R, et al. Elevated cerebrospinal fluid neurofilament light levels in patients with amyotrophic lateral sclerosis: a possible marker of disease severity and progression. European journal of neurology 2012;19:1561-1567.
47. Hu Y-Y, He S-S, Wang X-C, et al. Elevated levels of phosphorylated neurofilament proteins in cerebrospinal fluid of Alzheimer disease patients. Neuroscience letters 2002;320:156-160.
48. Zetterberg H, Skillbäck T, Mattsson N, et al. Association of cerebrospinal fluid neurofilament light concentration with Alzheimer disease progression. JAMA neurology 2016;73:60-67.
49. Skillbäck T, Farahmand B, Bartlett JW, et al. CSF neurofilament light differs in neurodegenerative diseases and predicts severity and survival. Neurology 2014;83:1945-1953.
50. Trojanowski J, Walkenstein N, Lee V. Expression of neurofilament subunits in neurons of the central and peripheral nervous system: an immunohistochemical study with monoclonal antibodies. Journal of Neuroscience 1986;6:650-660.
51. Alvarez-Bolado G, Rodríguez-Sánchez P, Tejero-Díez P, Fairen A, Díez-Guerra FJ. Neurogranin in the development of the rat telencephalon. Neuroscience 1996;73:565-580.
52. Bogdanovic N, Davidsson P, Gottfries J, Volkman I, Winblad B, Blennow K. Regional and cellular distribution of synaptic proteins in the normal human brain. Brain Aging 2002;2:18-30.
53. Huang K-P, Huang FL, Jäger T, Li J, Reymann KG, Balschun D. Neurogranin/RC3 enhances long-term potentiation and learning by promoting calcium-mediated signaling. Journal of Neuroscience 2004;24:10660-10669.
54. Masliah E, Mallory M, Hansen L, Richard D, Alford M, Terry R. Synaptic and neuritic alterations during the progression of Alzheimer's disease. Neuroscience letters 1994;174:67-72.

55. Scheff SW, Price DA. Synaptic pathology in Alzheimer's disease: a review of ultrastructural studies. Neurobiology of aging 2003;24:1029-1046.
56. Hamos JE, DeGennaro LJ, Drachman DA. Synaptic loss in Alzheimer's disease and other dementias. Neurology 1989;39:355-355.
57. DeKosky ST, Scheff SW, Styren SD. Structural correlates of cognition in dementia: quantification and assessment of synapse change. Neurodegeneration 1996;5:417-421.
58. Reddy PH, Mani G, Park BS, et al. Differential loss of synaptic proteins in Alzheimer's disease: implications for synaptic dysfunction. Journal of Alzheimer's Disease 2005;7:103-117.
59. Tarawneh R, D'Angelo G, Crimmins D, et al. Diagnostic and prognostic utility of the synaptic marker neurogranin in Alzheimer disease. JAMA neurology 2016;73:561-571.
60. Kester MI, Teunissen CE, Crimmins DL, et al. Neurogranin as a cerebrospinal fluid biomarker for synaptic loss in symptomatic Alzheimer disease. JAMA neurology 2015;72:1275-1280.
61. Wellington H, Paterson RW, Portelius E, et al. Increased CSF neurogranin concentration is specific to Alzheimer disease. Neurology 2016;86:829-835.
62. Bobinski M, De Leon M, Wegiel J, et al. The histological validation of post mortem magnetic resonance imaging-determined hippocampal volume in Alzheimer's disease. Neuroscience 1999;95:721-725.
63. Convit A, De Leon M, Tarshish C, et al. Specific hippocampal volume reductions in individuals at risk for Alzheimer's disease. Neurobiology of aging 1997;18:131-138.
64. Schuff N, Woerner N, Boreta L, et al. MRI of hippocampal volume loss in early Alzheimer's disease in relation to ApoE genotype and biomarkers. Brain 2009;132:1067-1077.
65. Baron J, Chetelat G, Desgranges B, et al. In vivo mapping of gray matter loss with voxel-based morphometry in mild Alzheimer's disease. Neuroimage 2001;14:298-309.
66. Du A-T, Schuff N, Kramer JH, et al. Different regional patterns of cortical thinning in Alzheimer's disease and frontotemporal dementia. Brain 2007;130:1159-1166.
67. Scheltens P, Barkhof F, Leys D, Wolters EC, Ravid R, Kamphorst W. Histopathologic correlates of white matter changes on MRI in Alzheimer's disease and normal aging. Neurology 1995;45:883-888.
68. Takahashi S, Yonezawa H, Takahashi J, Kudo M, Inoue T, Tohgi H. Selective reduction of diffusion anisotropy in white matter of Alzheimer disease brains measured by 3.0 Tesla magnetic resonance imaging. Neuroscience letters 2002;332:45-48.
69. Huang J, Friedland R, Auchus A. Diffusion tensor imaging of normal-appearing white matter in mild cognitive impairment and early Alzheimer disease: preliminary evidence of axonal degeneration in the temporal lobe. American Journal of Neuroradiology 2007;28:1943-1948.
70. Zhuang L, Sachdev PS, Trollor JN, et al. Microstructural white matter changes, not hippocampal atrophy, detect early amnestic mild cognitive impairment. PloS one 2013;8:e58887.
71. Canu E, McLaren DG, Fitzgerald ME, et al. Microstructural diffusion changes are independent of macrostructural volume loss in moderate to severe Alzheimer's disease. Journal of Alzheimer's Disease 2010;19:963-976.
72. Amlien I, Fjell A. Diffusion tensor imaging of white matter degeneration in Alzheimer's disease and mild cognitive impairment. Neuroscience 2014;276:206-215.
73. Sachdev PS, Zhuang L, Braidy N, Wen W. Is Alzheimer's a disease of the white matter? Current opinion in psychiatry 2013;26:244-251.

74. Madden DJ, Whiting WL, Huettel SA, White LE, MacFall JR, Provenzale JM. Diffusion tensor imaging of adult age differences in cerebral white matter: relation to response time. Neuroimage 2004;21:1174-1181.
75. Salat DH, Tuch DS, Greve DN, et al. Age-related alterations in white matter microstructure measured by diffusion tensor imaging. Neurobiol Aging 2005;26:1215-1227.
76. Charlton R, Barrick T, McIntyre D, et al. White matter damage on diffusion tensor imaging correlates with age-related cognitive decline. Neurology 2006;66:217-222.
77. Sullivan EV, Pfefferbaum A. Diffusion tensor imaging and aging. Neurosci Biobehav Rev 2006;30:749-761.
78. Bendlin BB, Fitzgerald ME, Ries ML, et al. White matter in aging and cognition: a cross-sectional study of microstructure in adults aged eighteen to eighty-three. Developmental neuropsychology 2010;35:257-277.
79. Nazeri A, Chakravarty MM, Rajji TK, et al. Superficial white matter as a novel substrate of age-related cognitive decline. Neurobiol Aging 2015a;36:2094-2106.
80. Gold BT, Zhu Z, Brown CA, et al. White matter integrity is associated with cerebrospinal fluid markers of Alzheimer's disease in normal adults. Neurobiology of aging 2014;35:2263-2271.
81. Hoy AR, Ly M, Carlsson CM, et al. Microstructural white matter alterations in preclinical Alzheimer's disease detected using free water elimination diffusion tensor imaging. PloS one 2017;12:e0173982.
82. Dean DC, Hurley SA, Kecskemeti SR, et al. Association of Amyloid Pathology With Myelin Alteration in Preclinical Alzheimer Disease. JAMA neurology 2017;74:41-49.
83. Blasko I, Stampfer-Kountchev M, Robatscher P, Veerhuis R, Eikelenboom P, Grubeck-Loebenstein B. How chronic inflammation can affect the brain and support the development of Alzheimer's disease in old age: the role of microglia and astrocytes. Aging cell 2004;3:169-176.
84. Block ML, Hong J-S. Microglia and inflammation-mediated neurodegeneration: multiple triggers with a common mechanism. Progress in neurobiology 2005;76:77-98.
85. Sutphen CL, Jasielec MS, Shah AR, et al. Longitudinal cerebrospinal fluid biomarker changes in preclinical Alzheimer disease during middle age. JAMA neurology 2015;72:1029-1042.
86. Antonell A, Mansilla A, Rami L, et al. Cerebrospinal fluid level of YKL-40 protein in preclinical and prodromal Alzheimer's disease. Journal of Alzheimer's Disease 2014;42:901-908.
87. Craig-Schapiro R, Perrin RJ, Roe CM, et al. YKL-40: a novel prognostic fluid biomarker for preclinical Alzheimer's disease. Biological psychiatry 2010;68:903-912.
88. Rosén C, Andersson C-H, Andreasson U, et al. Increased levels of chitotriosidase and YKL-40 in cerebrospinal fluid from patients with Alzheimer's disease. Dementia and geriatric cognitive disorders extra 2014;4:297-304.
89. Olsson B, Hertze J, Lautner R, et al. Microglial markers are elevated in the prodromal phase of Alzheimer's disease and vascular dementia. Journal of Alzheimer's Disease 2013;33:45-53.
90. Jones DK, Knösche TR, Turner R. White matter integrity, fiber count, and other fallacies: the do's and don'ts of diffusion MRI. Neuroimage 2013;73:239-254.
91. Lemkaddem A, Daducci A, Kunz N, et al. Connectivity and tissue microstructural alterations in right and left temporal lobe epilepsy revealed by diffusion spectrum imaging. NeuroImage: Clinical 2014;5:349-358.
92. Wen Q, Kelley DA, Banerjee S, et al. Clinically feasible NODDI characterization of glioma using multiband EPI at 7T. NeuroImage: Clinical 2015.

93. Figini M, Baselli G, Riva M, Bello L, Zhang H, Bizzi A. NODDI performs better than DTI in brain tumors with vasogenic edema. Proc Intl Soc Mag Reson Med; 2014: 0271.
94. Eaton-Rosen Z, Melbourne A, Orasanu E, et al. Longitudinal measurement of the developing grey matter in preterm subjects using multi-modal MRI. NeuroImage 2015;111:580-589.
95. Kunz N, Zhang H, Vasung L, et al. Assessing white matter microstructure of the newborn with multi-shell diffusion MRI and biophysical compartment models. Neuroimage 2014;96:288-299.
96. Nazeri A, Chakravarty MM, Rotenberg DJ, et al. Functional Consequences of Neurite Orientation Dispersion and Density in Humans across the Adult Lifespan. The Journal of Neuroscience 2015;35:1753-1762.
97. Billiet T, Vandenbulcke M, Madler B, et al. Age-related microstructural differences quantified using myelin water imaging and advanced diffusion MRI. Neurobiol Aging 2015;36:2107-2121.
98. Jelescu IO, Veraart J, Adisetiyo V, Milla SS, Novikov DS, Fieremans E. One diffusion acquisition and different white matter models: how does microstructure change in human early development based on WMTI and NODDI? Neuroimage 2015;107:242-256.
99. Magnollay L, Grussu F, Wheeler-Kingshott CA, et al. An investigation of brain neurite density and dispersion in multiple sclerosis using single shell diffusion imaging. brain 2014;61:1000-1016.
100. Adluru G, Gur Y, Anderson JS, Richards LG, Adluru N, DiBella EV. Assessment of white matter microstructure in stroke patients using NODDI. Engineering in Medicine and Biology Society (EMBC), 2014 36th Annual International Conference of the IEEE; 2014: IEEE: 742-745.
101. Stikov N, Campbell JS, Stroh T, et al. In vivo histology of the myelin g-ratio with magnetic resonance imaging. NeuroImage 2015.
102. Merluzzi AP, Dean DC, Adluru N, et al. Age-dependent differences in brain tissue microstructure assessed with neurite orientation dispersion and density imaging. Neurobiology of aging 2016;43:79-88.
103. Kodiweera C, Alexander AL, Harezlak J, McAllister TW, Wu Y-C. Age effects and sex differences in human brain white matter of young to middle-aged adults: A DTI, NODDI, and q-space study. NeuroImage 2015.
104. Clark LR, Racine AM, Koscik RL, et al. Beta-amyloid and cognitive decline in late middle age: findings from the Wisconsin Registry for Alzheimer's Prevention study. Alzheimer's & dementia: the journal of the Alzheimer's Association 2016;12:805-814.
105. Weintraub S, Salmon D, Mercaldo N, et al. The Alzheimer's disease centers' uniform data set (UDS): The neuropsychological test battery. Alzheimer disease and associated disorders 2009;23:91.
106. McKhann GM, Knopman DS, Chertkow H, et al. The diagnosis of dementia due to Alzheimer's disease: Recommendations from the National Institute on Aging-Alzheimer's Association workgroups on diagnostic guidelines for Alzheimer's disease. Alzheimer's & dementia 2011;7:263-269.
107. Starks EJ, Patrick O'Grady J, Hoscheidt SM, et al. Insulin Resistance is Associated with Higher Cerebrospinal Fluid Tau Levels in Asymptomatic APOEε4 Carriers. Journal of Alzheimer's Disease 2015;46:525-533.

108. Smach MA, Charfeddine B, Ben Othman L, et al. Evaluation of cerebrospinal fluid tau/beta-amyloid (42) ratio as diagnostic markers for Alzheimer disease. European neurology 2009;62:349-355.
109. Hansson O, Zetterberg H, Vanmechelen E, et al. Evaluation of plasma Aβ 40 and Aβ 42 as predictors of conversion to Alzheimer's disease in patients with mild cognitive impairment. Neurobiology of aging 2010;31:357-367.
110. Mattsson N, Insel PS, Palmqvist S, et al. Cerebrospinal fluid tau, neurogranin, and neurofilament light in Alzheimer's disease. EMBO molecular medicine 2016;8:1184-1196.
111. Janelidze S, Zetterberg H, Mattsson N, et al. CSF Aβ42/Aβ40 and Aβ42/Aβ38 ratios: better diagnostic markers of Alzheimer disease. Annals of clinical and translational neurology 2016.
112. Fagan AM, Roe CM, Xiong C, Mintun MA, Morris JC, Holtzman DM. Cerebrospinal fluid tau/β-amyloid42 ratio as a prediction of cognitive decline in nondemented older adults. Archives of neurology 2007;64:343-349.
113. Skillbäck T, Mattsson N, Blennow K, Zetterberg H. Cerebrospinal fluid neurofilament light concentration in motor neuron disease and frontotemporal dementia predicts survival. Amyotrophic Lateral Sclerosis and Frontotemporal Degeneration 2017;18:397-403.
114. Díez-Guerra FJ. Neurogranin, a link between calcium/calmodulin and protein kinase C signaling in synaptic plasticity. IUBMB life 2010;62:597-606.
115. Davidsson P, Blennow K. Neurochemical dissection of synaptic pathology in Alzheimer's disease. International psychogeriatrics 1998;10:11-23.
116. Wildsmith KR, Schauer SP, Smith AM, et al. Identification of longitudinally dynamic biomarkers in Alzheimer's disease cerebrospinal fluid by targeted proteomics. Molecular neurodegeneration 2014;9:22.
117. Choi J, Lee H-W, Suk K. Plasma level of chitinase 3-like 1 protein increases in patients with early Alzheimer's disease. Journal of neurology 2011;258:2181-2185.
118. Sekar S, McDonald J, Cuyugan L, et al. Alzheimer's disease is associated with altered expression of genes involved in immune response and mitochondrial processes in astrocytes. Neurobiology of aging 2015;36:583-591.
119. Van Eldik LJ, Carrillo MC, Cole PE, et al. The roles of inflammation and immune mechanisms in Alzheimer's disease. Alzheimer's & Dementia: Translational Research & Clinical Interventions 2016;2:99-109.
120. Katzman R. Education and the prevalence of dementia and Alzheimer's disease. Neurology 1993.
121. Roe CM, Xiong C, Miller JP, Morris JC. Education and Alzheimer disease without dementia support for the cognitive reserve hypothesis. Neurology 2007;68:223-228.
122. Norton S, Matthews FE, Barnes DE, Yaffe K, Brayne C. Potential for primary prevention of Alzheimer's disease: an analysis of population-based data. The Lancet Neurology 2014;13:788-794.
123. Lee S, Viqar F, Zimmerman ME, et al. White matter hyperintensities are a core feature of Alzheimer's disease: evidence from the dominantly inherited Alzheimer network. Annals of neurology 2016;79:929-939.
124. Zhang B, Xu Y, Zhu B, Kantarci K. The role of diffusion tensor imaging in detecting microstructural changes in prodromal Alzheimer's disease. CNS neuroscience & therapeutics 2014;20:3-9.
125. Doan NT, Engvig A, Persson K, et al. Dissociable diffusion MRI patterns of white matter microstructure and connectivity in Alzheimer's disease spectrum. Scientific reports 2017;7:45131.

126. Wu Y-C, Alexander AL. Hybrid diffusion imaging. NeuroImage 2007;36:617-629.
127. Zhang H, Schneider T, Wheeler-Kingshott CA, Alexander DC. NODDI: practical in vivo neurite orientation dispersion and density imaging of the human brain. Neuroimage 2012;61:1000-1016.
128. Caverzasi E, Papinutto N, Castellano A, et al. Neurite orientation dispersion and density imaging color maps to characterize brain diffusion in neurologic disorders. Journal of Neuroimaging 2016;26:494-498.
129. Timmers I, Roebroeck A, Bastiani M, Jansma B, Rubio-Gozalbo E, Zhang H. Assessing Microstructural Substrates of White Matter Abnormalities: A Comparative Study Using DTI and NODDI. PloS one 2016;11:e0167884.
130. Johnson SC, Koscik RL, Jonaitis EM, et al. The Wisconsin Registry for Alzheimer's Prevention: A Review of findings and current directions. Alzheimer's & Dementia: Diagnosis, Assessment & Disease Monitoring 2017.
131. Kawas C, Segal J, Stewart WF, Corrada M, Thal LJ. A validation study of the Dementia Questionnaire. Archives of Neurology 1994;51:901-906.
132. Racine AM, Koscik RL, Nicholas CR, et al. Cerebrospinal fluid ratios with Aβ 42 predict preclinical brain β-amyloid accumulation. Alzheimer's & Dementia: Diagnosis, Assessment & Disease Monitoring 2016;2:27-38.
133. Hansson O, Zetterberg H, Buchhave P, Londos E, Blennow K, Minthon L. Association between CSF biomarkers and incipient Alzheimer's disease in patients with mild cognitive impairment: a follow-up study. The Lancet Neurology 2006;5:228-234.
134. Johnson SC, Christian BT, Okonkwo OC, et al. Amyloid burden and neural function in people at risk for Alzheimer's Disease. Neurobiology of aging 2014;35:576-584.
135. Sprecher KE, Bendlin BB, Racine AM, et al. Amyloid burden is associated with self-reported sleep in nondemented late middle-aged adults. Neurobiology of aging 2015;36:2568-2576.
136. Racine AM, Clark LR, Berman SE, et al. Associations between performance on an abbreviated CogState battery, other measures of cognitive function, and biomarkers in people at risk for Alzheimer's disease. Journal of Alzheimer's Disease 2016;54:1395-1408.
137. Andersson JL, Sotiropoulos SN. An integrated approach to correction for off-resonance effects and subject movement in diffusion MR imaging. NeuroImage 2016;125:1063-1078.
138. Smith SM. Fast robust automated brain extraction. Human brain mapping 2002;17:143-155.
139. Jenkinson M, Bannister P, Brady M, Smith S. Improved optimization for the robust and accurate linear registration and motion correction of brain images. Neuroimage 2002;17:825-841.
140. Varentsova A, Zhang S, Arfanakis K. Development of a high angular resolution diffusion imaging human brain template. NeuroImage 2014;91:177-186.
141. Mito R, Raffelt D, Dhollander T, et al. Fibre-specific white matter reductions in Alzheimer's disease and mild cognitive impairment. Brain 2018;141:888-902.
142. Perani D. FDG-PET and amyloid-PET imaging: the diverging paths. Current opinion in neurology 2014;27:405-413.
143. Jacobs HI, Hedden T, Schultz AP, et al. Structural tract alterations predict downstream tau accumulation in amyloid-positive older individuals. Nature neuroscience 2018:1.
144. Racine AM, Merluzzi AP, Adluru N, et al. Association of longitudinal white matter degeneration and cerebrospinal fluid biomarkers of neurodegeneration, inflammation and Alzheimer's disease in late-middle-aged adults. Brain Imaging and Behavior 2017:1-12.

145. Zetterberg H, Skillbäck T, Mattsson N, et al. Association of Cerebrospinal Fluid Neurofilament Light Concentration With Alzheimer Disease Progression. JAMA neurology 2015:1-8.
146. Janelidze S, Hertze J, Zetterberg H, et al. Cerebrospinal fluid neurogranin and YKL-40 as biomarkers of Alzheimer's disease. Annals of clinical and translational neurology 2016;3:12-20.
147. Kvartsberg H, Portelius E, Andreasson U, et al. Characterization of the postsynaptic protein neurogranin in paired cerebrospinal fluid and plasma samples from Alzheimer's disease patients and healthy controls. Alzheimer's research & therapy 2015;7:1-9.
148. Jeurissen B, Leemans A, Tournier JD, Jones DK, Sijbers J. Investigating the prevalence of complex fiber configurations in white matter tissue with diffusion magnetic resonance imaging. Human brain mapping 2013;34:2747-2766.
149. Slattery CF, Zhang J, Paterson RW, et al. ApoE influences regional white-matter axonal density loss in Alzheimer's disease. Neurobiology of Aging 2017;57:8-17.
150. Colgan N, Siow B, O'Callaghan JM, et al. Application of neurite orientation dispersion and density imaging (NODDI) to a tau pathology model of Alzheimer's disease. NeuroImage 2016;125:739-744.
151. Chang YS, Owen JP, Pojman NJ, et al. White Matter Changes of Neurite Density and Fiber Orientation Dispersion during Human Brain Maturation. PloS one 2015;10:e0123656.
152. Grussu F, Schneider T, Zhang H, Alexander DC, Wheeler–Kingshott CA. Neurite orientation dispersion and density imaging of the healthy cervical spinal cord in vivo. NeuroImage 2015;111:590-601.
153. Zetterberg H. Tauomics and Kinetics in Human Neurons and Biological Fluids. Neuron 2018;97:1202-1205.
154. Wang Y, Gupta A, Liu Z, et al. DTI registration in atlas based fiber analysis of infantile Krabbe disease. Neuroimage 2011;55:1577-1586.
155. Zhang H, Yushkevich PA, Alexander DC, Gee JC. Deformable registration of diffusion tensor MR images with explicit orientation optimization. Medical image analysis 2006;10:764-785.
156. Adluru N, Zhang H, Fox AS, et al. A diffusion tensor brain template for rhesus macaques. Neuroimage 2012;59:306-318.
157. Schmidt P, Gaser C, Arsic M, et al. An automated tool for detection of FLAIR-hyperintense white-matter lesions in multiple sclerosis. Neuroimage 2012;59:3774-3783.
158. Keihaninejad S, Heckemann RA, Fagiolo G, et al. A robust method to estimate the intracranial volume across MRI field strengths (1.5 T and 3T). Neuroimage 2010;50:1427-1437.
159. Jack CR, Bennett DA, Blennow K, et al. A/T/N: An unbiased descriptive classification scheme for Alzheimer disease biomarkers. Neurology 2016;87:539-547.
160. Jack Jr CR, Bennett DA, Blennow K, et al. NIA-AA Research Framework: Toward a biological definition of Alzheimer's disease. Alzheimer's & Dementia 2018;14:535-562.
161. Lista S, Toschi N, Baldacci F, et al. Diagnostic accuracy of CSF neurofilament light chain protein in the biomarker-guided classification system for Alzheimer's disease. Neurochemistry international 2017;108:355-360.
162. Tarawneh R, Head D, Allison S, et al. Cerebrospinal Fluid Markers of Neurodegeneration and Rates of Brain Atrophy in Early Alzheimer Disease. JAMA Neurol 2015;72:656-665.
163. Donohue MC, Sperling RA, Salmon DP, et al. The preclinical Alzheimer cognitive composite: measuring amyloid-related decline. JAMA neurology 2014;71:961-970.

164. Schmidt M. Rey auditory verbal learning test: a handbook: Western Psychological Services Los Angeles, 1996.
165. Wechsler D. WMS-R: Wechsler memory scale-revised: Psychological Corporation, 1987.
166. Wechsler D. WAIS-R manual: Wechsler adult intelligence scale-revised: Psychological Corporation, 1981.
167. Folstein MF, Folstein SE, McHugh PR. "Mini-mental state": a practical method for grading the cognitive state of patients for the clinician. Journal of psychiatric research 1975;12:189-198.
168. Grober E, Hall CB, Lipton RB, Zonderman AB, Resnick SM, Kawas C. Memory impairment, executive dysfunction, and intellectual decline in preclinical Alzheimer's disease. Journal of the International Neuropsychological Society 2008;14:266-278.
169. Benedict RH. Brief visuospatial memory test--revised: professional manual: PAR, 1997.
170. Reitan R, Wolfson D. The Halstead-Reitan neuropsychological test battery: therapy and clinical assessment. Tucson, AZ: Neuropsychological Press, 1985.
171. Trenerry M, Crosson B, DeBoe J, Leber W. Stroop Neuropsychological Screening Test. Odessa, FL: Psychological Assessment Resources. Inc, 1989.
172. Bates D, Mächler M, Bolker B, Walker S. Fitting linear mixed-effects models using lme4. arXiv preprint arXiv:14065823 2014.
173. Clark LR, Berman SE, Norton D, et al. Age-accelerated cognitive decline in asymptomatic adults with CSF β-amyloid. Neurology 2018:10.1212/WNL. 0000000000005291.
174. Wilkinson GS. WRAT-3: Wide range achievement test administration manual: Wide Range, Incorporated, 1993.
175. Blennow K, Dubois B, Fagan AM, Lewczuk P, de Leon MJ, Hampel H. Clinical utility of cerebrospinal fluid biomarkers in the diagnosis of early Alzheimer's disease. Alzheimer's & Dementia 2015;11:58-69.
176. Casaletto KB, Elahi FM, Bettcher BM, et al. Neurogranin, a synaptic protein, is associated with memory independent of Alzheimer biomarkers. Neurology 2017;89:1782-1788.
177. Kvartsberg H, Duits FH, Ingelsson M, et al. Cerebrospinal fluid levels of the synaptic protein neurogranin correlates with cognitive decline in prodromal Alzheimer's disease. Alzheimer's & Dementia 2015;11:1180-1190.
178. Headley A, De Leon-Benedetti A, Dong C, et al. Neurogranin as a predictor of memory and executive function decline in MCI patients. Neurology 2018;90:e887-e895.
179. Pereira JB, Westman E, Hansson O. Association between cerebrospinal fluid and plasma neurodegeneration biomarkers with brain atrophy in Alzheimer's disease. Neurobiology of aging 2017;58:14-29.
180. Hall S, Öhrfelt A, Constantinescu R, et al. Accuracy of a panel of 5 cerebrospinal fluid biomarkers in the differential diagnosis of patients with dementia and/or parkinsonian disorders. Archives of neurology 2012;69:1445-1452.
181. Schoonenboom N, Reesink F, Verwey N, et al. Cerebrospinal fluid markers for differential dementia diagnosis in a large memory clinic cohort. Neurology 2012;78:47-54.
182. Aerts MB, Esselink RA, Claassen JA, Abdo WF, Bloem BR, Verbeek MM. CSF Tau, Aβ 42, and MHPG Differentiate Dementia with Lewy Bodies from Alzheimer's Disease. Journal of Alzheimer's Disease 2011;27:377-384.
183. Magalhães CA, Figueiró M, Fraga VG, et al. Cerebrospinal fluid biomarkers for the differential diagnosis of Alzheimer's disease. Jornal Brasileiro de Patologia e Medicina Laboratorial 2015;51:376-382.

184. Paterson RW, Slattery CF, Poole T, et al. Cerebrospinal fluid in the differential diagnosis of Alzheimer's disease: clinical utility of an extended panel of biomarkers in a specialist cognitive clinic. Alzheimer's research & therapy 2018;10:32.
185. Portelius E, Olsson B, Höglund K, et al. Cerebrospinal fluid neurogranin concentration in neurodegeneration: relation to clinical phenotypes and neuropathology. Acta Neuropathologica 2018:1-14.
186. Maia LF, Kaeser SA, Reichwald J, et al. Changes in amyloid-β and Tau in the cerebrospinal fluid of transgenic mice overexpressing amyloid precursor protein. Science translational medicine 2013;5:194re192-194re192.
187. Sato C, Barthélemy NR, Mawuenyega KG, et al. Tau kinetics in neurons and the human central nervous system. Neuron 2018;97:1284-1298. e1287.
188. Guo T, Brendel M, Grimmer T, Rominger A, Yakushev I. Baseline amyloid PET predicts spatial pattern of beta-amyloid accumulation over time. Journal of Nuclear Medicine 2016;57:510-510.
189. Villemagne VL, Burnham S, Bourgeat P, et al. Amyloid β deposition, neurodegeneration, and cognitive decline in sporadic Alzheimer's disease: a prospective cohort study. The Lancet Neurology 2013;12:357-367.
190. Jack Jr CR, Wiste HJ, Vemuri P, et al. Brain beta-amyloid measures and magnetic resonance imaging atrophy both predict time-to-progression from mild cognitive impairment to Alzheimer's disease. Brain 2010;133:3336-3348.
191. Santos AN, Ewers M, Minthon L, et al. Amyloid-β oligomers in cerebrospinal fluid are associated with cognitive decline in patients with Alzheimer's disease. Journal of Alzheimer's disease 2012;29:171-176.
192. Landau SM, Mintun MA, Joshi AD, et al. Amyloid deposition, hypometabolism, and longitudinal cognitive decline. Annals of neurology 2012;72:578-586.
193. Doraiswamy PM, Sperling RA, Coleman RE, et al. Amyloid-β assessed by florbetapir F 18 PET and 18-month cognitive decline A multicenter study. Neurology 2012;79:1636-1644.
194. Clark LR, Berman SE, Norton D, et al. Age-accelerated cognitive decline in asymptomatic adults with CSF beta-amyloid. Neurology 2018;90:e1306-e1315.
195. Finnema SJ, Nabulsi NB, Eid T, et al. Imaging synaptic density in the living human brain. Science translational medicine 2016;8:348ra396-348ra396.
196. Boots EA, Schultz SA, Almeida RP, et al. Occupational complexity and cognitive reserve in a middle-aged cohort at risk for Alzheimer's disease. Archives of Clinical Neuropsychology 2015;30:634-642.
197. Arenaza-Urquijo EM, Wirth M, Chételat G. Cognitive reserve and lifestyle: moving towards preclinical Alzheimer's disease. Frontiers in Aging Neuroscience 2015;7:134.
198. Ngandu T, Lehtisalo J, Solomon A, et al. A 2 year multidomain intervention of diet, exercise, cognitive training, and vascular risk monitoring versus control to prevent cognitive decline in at-risk elderly people (FINGER): a randomised controlled trial. The Lancet 2015;385:2255-2263.
199. Bartzokis G. Alzheimer's disease as homeostatic responses to age-related myelin breakdown. Neurobiology of aging 2011;32:1341-1371.
200. Fandos N, Pérez-Grijalba V, Pesini P, et al. Plasma amyloid β 42/40 ratios as biomarkers for amyloid β cerebral deposition in cognitively normal individuals. Alzheimer's & Dementia: Diagnosis, Assessment & Disease Monitoring 2017;8:179-187.

201. Lewczuk P, Matzen A, Blennow K, et al. Cerebrospinal Fluid Aβ 42/40 Corresponds Better than Aβ 42 to Amyloid PET in Alzheimer's Disease. Journal of Alzheimer's Disease 2017;55:813-822.
202. Palmqvist S, Mattsson N, Hansson O, Initiative AsDN. Cerebrospinal fluid analysis detects cerebral amyloid-β accumulation earlier than positron emission tomography. Brain 2016;139:1226-1236.
203. Blennow K, Zetterberg H. The past and the future of Alzheimer's disease CSF biomarkers—a journey toward validated biochemical tests covering the whole spectrum of molecular events. Frontiers in neuroscience 2015;9.
204. Snyder HM, Hendrix J, Bain LJ, Carrillo MC. Alzheimer's disease research in the context of the national plan to address Alzheimer's disease. Mol Aspects Med 2015.
205. Di Marco LY, Venneri A, Farkas E, Evans PC, Marzo A, Frangi AF. Vascular dysfunction in the pathogenesis of Alzheimer's disease—a review of endothelium-mediated mechanisms and ensuing vicious circles. Neurobiology of disease 2015;82:593-606.
206. Lois C, Gonzalez I, Johnson KA, Price JC. PET imaging of tau protein targets: a methodology perspective. Brain imaging and behavior 2018:1-12.
207. Mecca AP, Chen M-K, Naganawa M, et al. Initial Experience with PET Imaging of Synaptic Density (SV2A) in Alzheimer's Disease: A New Biomarker for Clinical Trials? The American Journal of Geriatric Psychiatry 2018;26:S145-S146.
208. Donat CK, Mirzaei N, Tang S-P, Edison P, Sastre M. Imaging of Microglial Activation in Alzheimer's Disease by [11 C] PBR28 PET. Biomarkers for Alzheimer's Disease Drug Development: Springer, 2018: 323-339.
209. Weuve J, Barnes LL, de Leon CFM, et al. Cognitive Aging in Black and White Americans: Cognition, Cognitive Decline, and Incidence of Alzheimer Disease Dementia. Epidemiology 2018;29:151-159.
210. Canevelli M, Bruno G, Vico C, et al. Socioeconomic disparities in clinical trials on Alzheimer's disease: a systematic review. European journal of neurology 2018.
211. Manly JJ. Deconstructing race and education for research on disparities in Alzheimer's disease and cognitive aging. Alzheimer's & Dementia: The Journal of the Alzheimer's Association 2015;11:P169-P170.